BRITISH ANTARCTIC SURVEY

SCIENTIFIC REPORTS

No. 66

CRUSTAL STRUCTURE OF THE SOUTH SHETLAND ISLANDS AND BRANSFIELD STRAIT

By

W. A. ASHCROFT, M.Sc., Ph.D.

Department of Geology, University of Birmingham

LONDON: PUBLISHED BY THE BRITISH ANTARCTIC SURVEY: 1972
NATURAL ENVIRONMENT RESEARCH COUNCIL

BRITISH ANTARCTIC SURVEY SCIENTIFIC REPORTS: No. 66

CRUSTAL STRUCTURE OF THE SOUTH SHETLAND ISLANDS AND BRANSFIELD STRAIT

By

W. A. ASHCROFT,* M.Sc., Ph.D.

Department of Geology, University of Birmingham

(Manuscript received 27th May, 1969)

ABSTRACT

THIS report describes marine seismic refraction investigations in the Bransfield Strait area of the Scotia arc. The geology and bathymetry of the area are summarized, and recording instrumentation and techniques are briefly described with special reference to the sono-radio buoy system used by the Department of Geology, University of Birmingham. The data and results from 13 reversed and seven unreversed marine seismic refraction lines are presented. The thickness and distribution of sediments are discussed, as well as the deeper crustal structure and the distribution of major faults.

The deepest layer encountered (7·6–7·7 km./sec.) has a velocity lower than that of normal mantle material. Beneath Bransfield Strait the crustal section is shown to be:

1·8 km. water	
2·5 km. sediments	(velocity 1·8–4·5 km./sec.)
1·0 km. rock	(velocity 5·3–5·6 km./sec.)
10·0 km. rock	(velocity 6·6 km./sec.)
Mantle	(velocity 7·6–7·7 km./sec.).

This structure extends as a narrow strip under the deep water (1·8 km.) of Bransfield Strait. On either side, beneath Trinity Peninsula to the south-east and the South Shetland Islands to the north-west, rocks with seismic velocities in the range 5·5–6·2 km./sec. thicken to 15–18 km. A major accumulation of sediment, up to 6 km. in thickness, has been found on the shelf north-west of the South Shetland Islands. Major east–west transcurrent faulting, probably involving rotation of blocks of crust, is shown to have been important in the Elephant and Clarence Islands group. An important zone of normal faulting is confirmed along the south-east side of the South Shetland Islands and there is evidence of similar normal faulting off the north-west coast of Trinity Peninsula.

This crustal structure is discussed in conjunction with the known geology and several modes of origin are considered. The hypothesis is put forward that the South Shetland Islands and the Antarctic Peninsula were once united. The (?) Carboniferous greywacke-facies sediments which occur on both the offshore islands and the Antarctic Peninsula are considered to have been deposited in the same trough which, as a single unit, underwent subsequent folding and plutonic intrusion. In Tertiary times a rift opened at the present site of Bransfield Strait as part of a regional process of continental drift, so that the South Shetland Islands became separated from the Antarctic Peninsula. Certain features of this structure are compared with the Red Sea rift.

* Present address: Department of Geology and Mineralogy, University of Aberdeen, Aberdeen.

CONTENTS

I. INTRODUCTION

THIS report describes the results of marine explosion seismic investigations conducted in the area of Bransfield Strait and the South Shetland Islands by personnel of the Department of Geology (Sub-Department of Geophysics), University of Birmingham, and the British Antarctic Survey.

The work was carried out at various times during the Antarctic summer seasons 1962–63, 1963–64 and 1964–65. Most of it was undertaken from the British Antarctic Survey vessel R.R.S. *Shackleton*, while H.M.S. *Protector* acted as "shot boat" during the two-ship seismic work.

The data on which this report is based comprise the seismic lines shown in Fig. 1. In addition, bathymetric and gravity data, and some results of total-field magnetic profiles in the area have been used to supplement the seismic information.

Previous geophysical work

The results of geophysical work carried out in this area have been described by Cox (1964) and Griffiths and others (1964). In their report on the results of gravity observations in this area, Griffiths and others showed an elongated gravity high, about 40 mgal in amplitude, over the South Shetland Islands, parallel to the trend of the islands and with a steep gradient to the south-east. This was interpreted in terms of faulting along the south-east side of the islands with a downthrow of several kilometres to the south-east, a structure supported by the present seismic investigations. A magnetic high was also found over the islands, again trending parallel to the arc and about 800 γ in amplitude. The anomaly is broad, clearly the result of a relatively deep source, and it was interpreted in terms of a ridge of trapezoidal cross-section centred under the islands and extending from about 5 to 20 km. in depth. The land–sea seismic lines in Bransfield Strait, reported by Griffiths and others as having been shot but not interpreted at the time of their publication, are incorporated in the present work.

Cox (1964) reported the results of five short (15 km.) two-ship seismic lines in north-east Bransfield Strait and he showed that the crust was unusual in possessing a high seismic velocity (6·4–7·1 km./sec.) at the relatively shallow depth of about 5 km. The present results indicate a rather smaller velocity range for rocks at this depth (6·5–6·9 km./sec.), and it is probable that the length of the earlier lines was insufficient to give a clearly determined velocity.

II. GEOLOGY

THE geology of Trinity Peninsula and the South Shetland Islands part of the Scotia arc is well known from field investigations over a long period (Wordie, 1921; Tyrrell, 1921, 1945; Adie, 1955, 1957, 1962, 1964; Hawkes, 1961*a*, *b*; Halpern, 1964; Aitkenhead, 1965; Barton, 1965; Elliot, 1965, 1966; Bibby, 1966; Hobbs, 1968), and therefore a redescription is unnecessary here.

The South Shetland Islands virtually mirror the geology of Trinity Peninsula. The oldest rocks are geosynclinal sediments closely comparable to the Trinity Peninsula Series, but they are only exposed over a small area of Livingston Island, where they dip steeply north-westwards. Old well-indurated volcanic rocks occur on Livingston Island but their relation to the geosynclinal sediments is not clear. They are also present on King George Island and in both islands they are older than the Andean batholiths, which form the central parts of the islands. On both Livingston and King George Islands considerable thicknesses of Tertiary lavas have been extruded from vents arranged in lines parallel to the length of the islands along both the north-west and south-east coasts, and marking the sites of tension faults. Both the faulting and the vulcanicity have apparently continued intermittently until Recent times.

The Elephant and Clarence Islands group, which is farther to the north-east, is relatively little known. Dynamically metamorphosed geosynclinal sediments striking east by north (parallel to the arc) and with a variable dip have been reported by Tyrrell (1945) on the north coast of Elephant Island. But at the extreme south end of the island there are marbles and amphibolites similar to those of the South Orkney Islands.

Tyrrell (1945) described albite-epidote-biotite-schists, which are probably andesitic in origin, from Clarence Island, whereas at Cornwallis Island (10 km. north-east of Elephant Island) there are (?) schists

comparable to those on the north coast of Elephant Island with an almost vertical dip and a strike 070–080°. Gibbs Island (27 km. south of Elephant Island) is composed of chlorite-albite-sericite-schists dipping to the south-west and striking parallel to the length of the island; there are schistose serpentinized dunites at the east end. Little is known of Aspland and O'Brien Islands, except that there are rocks with a planar structure, a steep dip and approximate north–south strike.

Although the detailed geology is little known, the repeated occurrence of metasediments of geosynclinal facies and the diversity of structural trends are points which stand out in the geology of the Elephant and Clarence Islands group. Previous accounts have emphasized the presence of high-grade metamorphic rocks and the absence of Tertiary lavas to stress the difference between these islands and the South Shetland Islands to the south-west.

III. BATHYMETRY

THE general features of the bathymetry of this area have been known since the voyages of R.R.S. *Discovery II* in the 1930's (Herdman, 1948). Many lines of soundings have been taken by R.R.S. *Shackleton* in recent years and these, together with soundings from the seismic lines and all available data on Admiralty Chart No. 3205 (South Shetland Islands and Bransfield Strait), have been contoured in Fig. 2. All soundings are from standard marine echo-sounding equipment and are uncorrected. The coverage is adequate over most of Bransfield Strait but it is poor at its north-east end, off the Trinity Peninsula coast and on the shelf and continental slope north-west of the South Shetland Islands.

The main feature of the area is the deep flat-bottomed trough beneath Bransfield Strait which is conveniently defined by the 1,000 m. isobath and referred to here as the "Bransfield Trough". Between Clarence and Bridgeman Islands this has an irregular bottom with at least one seamount with a relief of 1,800 m. and three separate basins of which the deepest reaches 2,800 m. Between Bridgeman and Deception Islands the bottom of the trough is invariably flat over wide areas, notably in the basin south-east of King George Island. Sub-bottom reflections on the echograms suggest that these areas are plains of sedimentation (Ashcroft, 1967). However, there are also considerable topographic features, for instance, the seamount south of King George Island. Where such features occur, the sea bed becomes rough, and this, together with the presence of magnetic anomalies over these features and the volcanic origin of Deception and Bridgeman Islands, leaves little doubt that they are submarine volcanoes. This view is also supported by their occurrence along a line joining Bridgeman and Deception Islands, and by the elongation along the same direction of two small features at about lat. 62°35′S., long. 58°50′W. Prior to this vulcanicity, the trough may have been a flat-bottomed feature either sloping gently from south-west to north-east or stepped down in three different levels of about 1,300, 1,850 and 2,900 m.

At its south-west end the trough is abruptly terminated by a steep slope leading up to a smooth, shallow shelf area. This shelf continues south-west of the present area towards Brabant and Anvers Islands and beyond with a width of between 100 and 150 km. defined by the 500 m. isobath. The steep slope terminating the "Bransfield Trough" trends north–south from Boyd Strait to the vincinity of Brabant Island, where there is a deep-water connection with Gerlache Strait (Herdman, 1948).

To the south of the trough proper, a complex shelf extends from the Trinity Peninsula coast, in places as far as 60 km. and at depths less than 200 m. This is broken by wide channels of deeper water with very rough and abrupt minor sea-bottom topography around a mean depth of 820 m. Tower Island (Fig. 2) is isolated from Trinity Peninsula by a particularly prominent feature of this type. In contrast, the surface of the elevated shelf is smooth, and the presence of the offshore islands and the numerous rocks and reefs which surround them (Montravel Rock, Zelée Rocks, etc.) shows that solid rock is everywhere near the sea bottom and that the shelves are probably erosional surfaces planed by wave action at a time of reduced sea-level. Indirect seismic evidence supports the view that there is little recent sediment on these shelves.

North-west of the South Shetland Islands is a smooth featureless shelf between 40 and 60 km. wide. In common with other Antarctic shelves, the break in slope is deep, at a depth of about 500 m. compared with a world average of about 130 m. Near the coast, the presence of numerous offshore islands and reefs indicates a rock platform of marine erosion, but farther offshore seismic evidence clearly shows that the shelf is the result of prolonged sedimentation which has built out a wedge of sediments along the side of the islands.

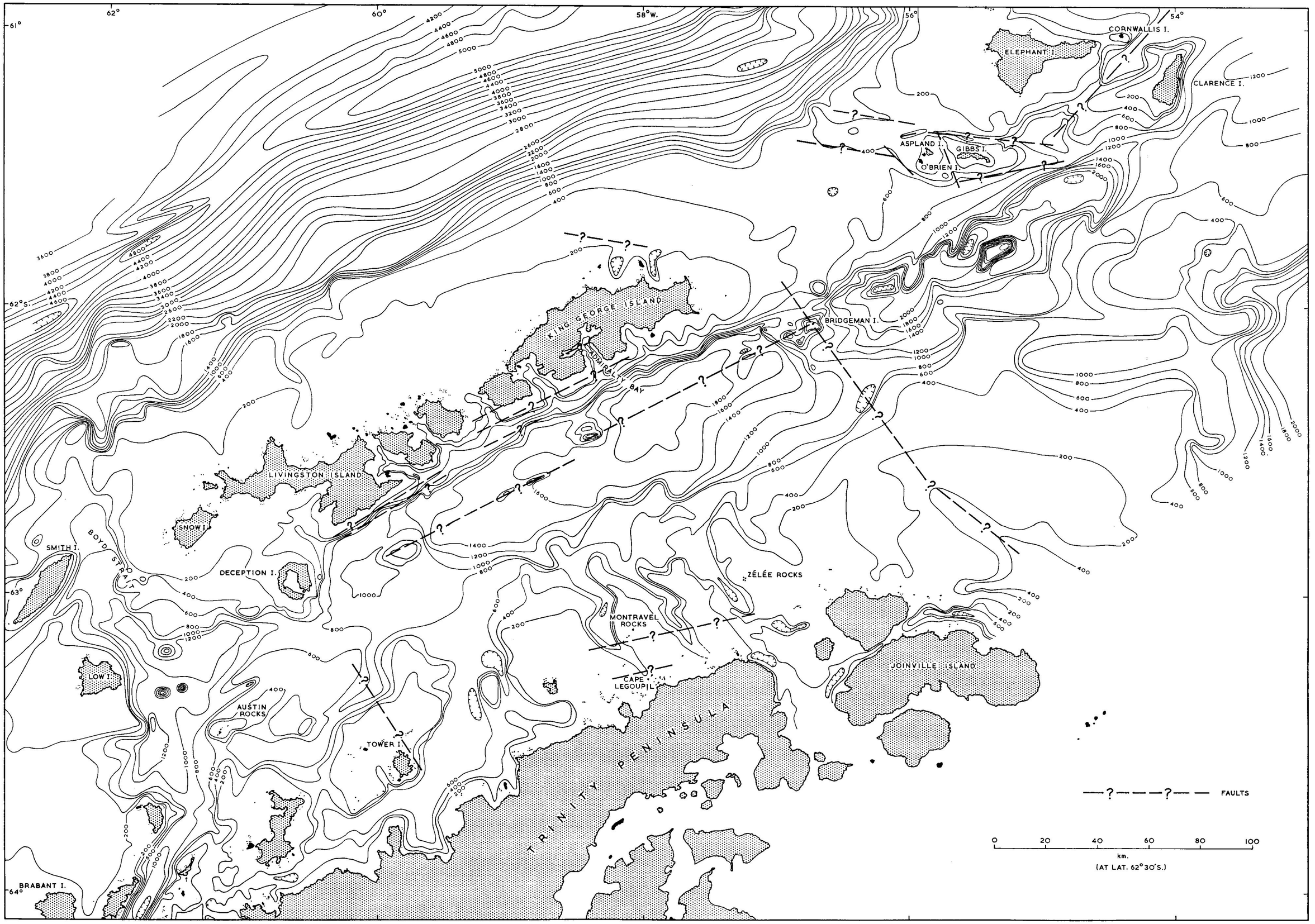

FIGURE 2

Bathymetric map of the South Shetland Islands–Bransfield Strait area. The positions of major faults are also shown. Bathymetric contours are at 200 m. intervals.

[face p. 5

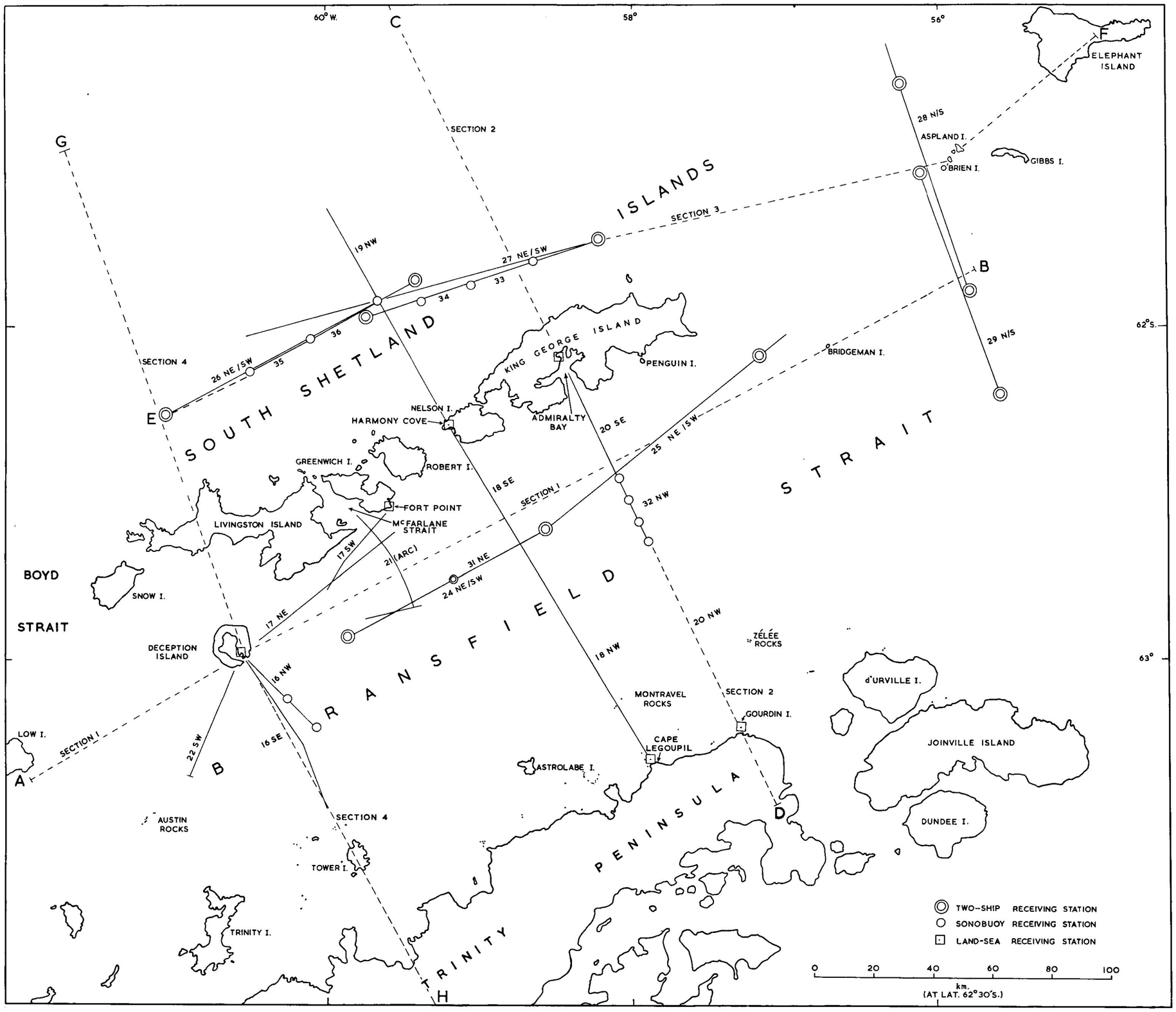

FIGURE 1

Map of the South Shetland Islands–Bransfield Strait area showing the locations of seismic lines. The broken lines A–B, etc. indicate the positions of the cross-sections (Figs. 31–34).

[face p. 4]

Around Elephant Island the shelf is again varied and the Gibbs Island group stands on an east–west ridge which noses out on the edge of the "Bransfield Trough". This will be shown later to be a fault-bounded block, and it seems likely that there is a close relationship between topography and structure in this area. Remarkably deep soundings (1,460–1,880 m.) have been recorded in what appears to be a deep cleft between Elephant and Clarence Islands (Fig. 2).

The continental slope to the north-west of the South Shetland Islands has an average gradient of about 5°. It shows considerable minor topography in places and leads down to a subdued but distinct trench. Maximum depths in this trench are in excess of 5·1 km. and the deepest parts are floored by a narrow flat plain.

IV. SEISMIC TECHNIQUES AND INSTRUMENTATION

THREE different types of seismic line are shown on Fig. 1—land–sea, two-ship and sonobuoy lines.

In land–sea shooting, a receiving station was set up at a convenient landing place and the ship dropped a line of explosive charges at increasing ranges out to sea. Where possible, these lines were reversed by setting up another receiving station at a point somewhere along the line and dropping a second set of charges in the reverse direction (e.g. Fig. 1, lines 18 and 20). There are two main drawbacks to this method: first, that sediment thicknesses away from land can never be determined, and secondly, that the line will inevitably cross major structures, thus increasing the complexity of the interpretation. This is essentially a reconnaissance technique of value in obtaining results when only one ship is available.

Two-ship shooting is a well-established marine seismic refraction technique (Shor, 1963) and the method used by the University of Birmingham group has already been described by Cox (1964) and Allen (1966). Two changes were introduced when carrying out the present work. A longer buoyant cable (457 m.) was used to ensure that the hydrophones were well away from ship noise. In addition, signals from two hydrophones, separately suspended at the end of the long buoyant cable, were mixed together in an attempt to improve the signal-to-noise ratio. To some extent, this measure was successful.

The instruments used in both the land–sea and the two-ship shooting have been described by Allen (1966), i.e. a 4-channel GTR-200 amplifier and filter system manufactured by Southwestern Industrial Electronics. An ultra-violet recorder was employed. Commercial refraction geophones were used in the land–sea work.

The technique of sonobuoy refraction shooting was first used by Hill (1952) in the North Atlantic Ocean soon after World War II and this has been used extensively by the Department of Geodesy and Geophysics, University of Cambridge (Hill, 1963). The University of Birmingham sonobuoy system was built by G. and E. Bradley Ltd., one of the Lucas Group, to our specification and first tested during the 1963–64 Antarctic field season. Circuit details of this system together with a review of the design considerations have already been published (Gurney, 1964), and only a brief account will be given here.

In Fig. 3 it can be seen that the hydrophone signal at the buoy was used to frequency-modulate a 5 kHz sub-carrier which was, in turn, transmitted to the ship as an amplitude-modulated 27 MHz radio signal. Transmitter power was approximately 1 W. At the ship terminal, the frequency-modulated sub-carrier was recorded on tape and at the same time demodulated to provide a monitor paper record of the seismic signal. Band-pass filtering on playback could be carried out through any external filter system and generally the filters from the GTR-200 system were used. Timing marks were provided by a crystal-controlled oscillator.

The buoy itself took the form of a galvanized steel drum about 0·9 m. high and 0·45 m. in diameter stabilized by a 5·4 m. keel, and the transistorized electronic units could be conveniently housed under the lid.

The maximum range achieved with this system was 50 km. Sensitivity was high, giving 10 Hz modulation on the sub-carrier for a 4 μV input at the hydrophone, and it was fully comparable to two-ship working under the same conditions. However, its dynamic range of 60 db was found to be insufficient to cope with the high-amplitude water wave, and this is evident in the representative set of records shown in Fig. 4. Ideally, the buoys should be used as a multiple-recording unit but generally circumstances, such as the time available and the prevailing weather conditions, determined the shooting configuration. A more detailed account of the field operations and the overall performance of the system has been given elsewhere (Ashcroft, 1967).

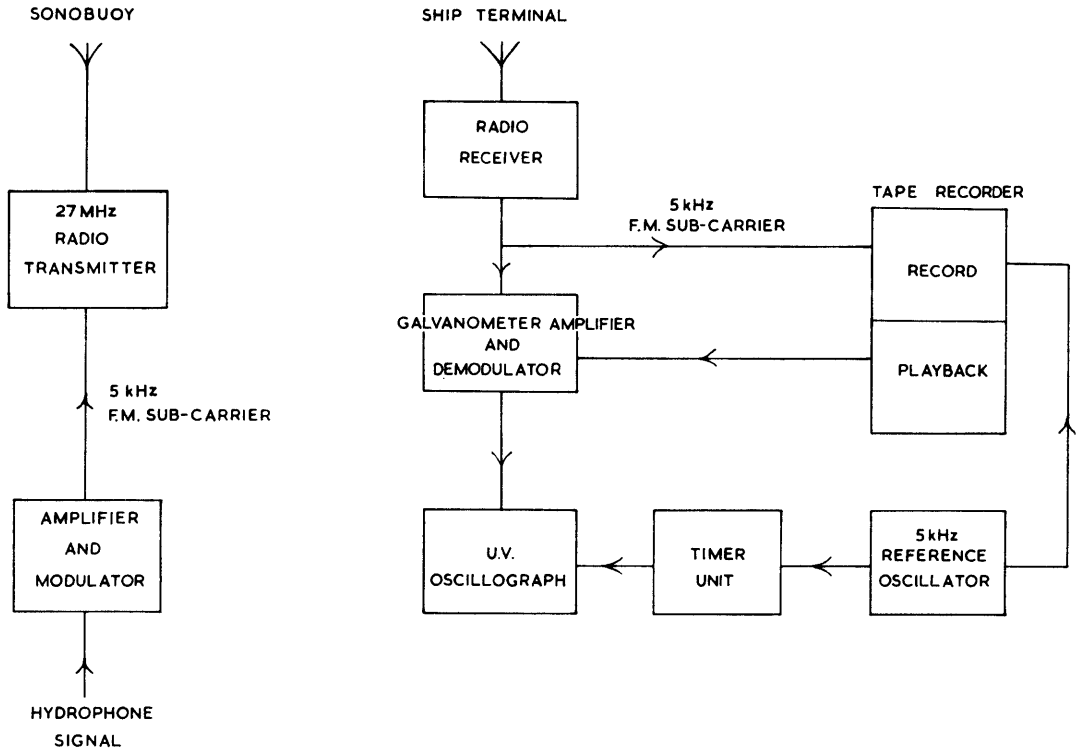

FIGURE 3

Diagrammatic representation of the sonobuoy system used in the seismic survey.

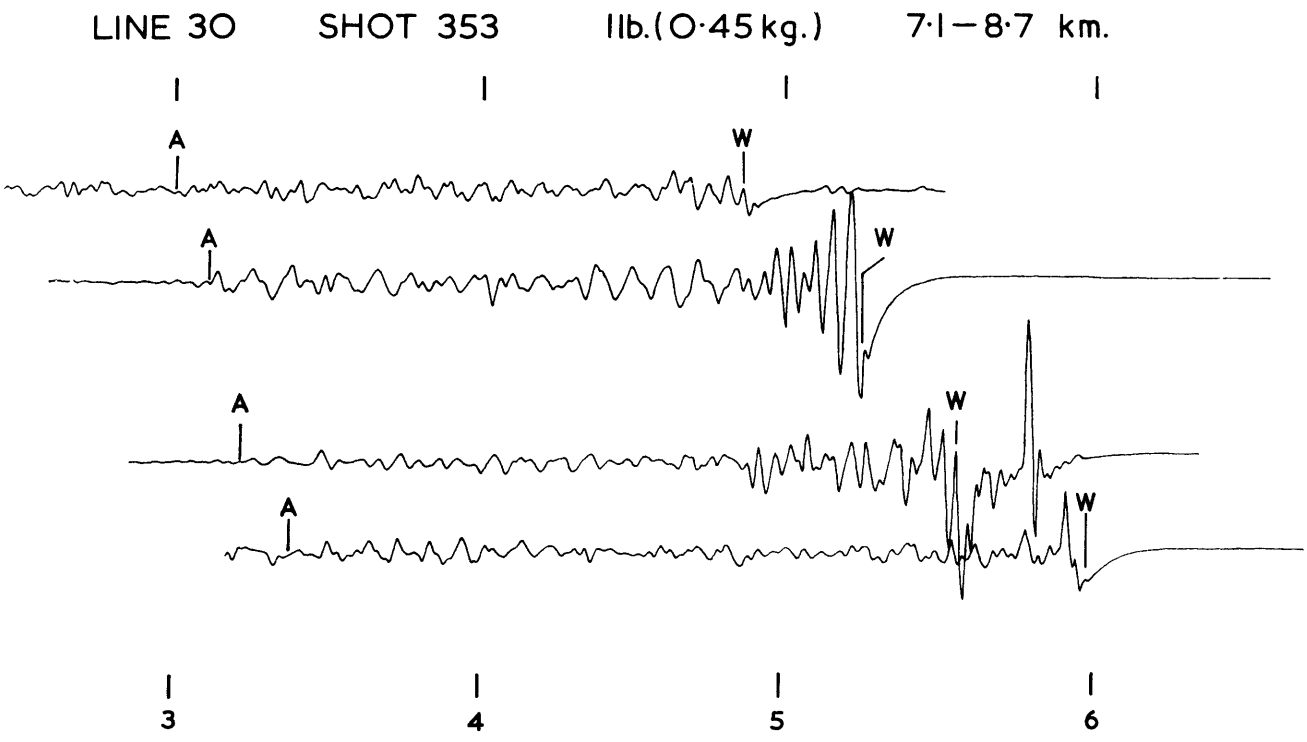

FIGURE 4

Seismic records of a single shot recorded on an in-line array of four sonobuoys. A, ground wave; W, water wave.

V. REDUCTION AND INTERPRETATION OF SEISMIC DATA

1. *Nature and quality of the seismic data*

Most of the records show clear first arrivals except at extreme ranges. Simple mixing of the signals of two hydrophones was found useful at times in enhancing the first break at great ranges.

Second arrivals were picked in considerable numbers on the two-ship and sonobuoy lines. Many of these, when plotted, proved to fall on lines parallel to the first arrivals from the main crustal layers and were probably reflected refractions. In particular, on one sonobuoy line it could be shown that a conspicuous set of second arrivals was of this type, arriving later than the first arrivals through being reflected once in the water layer immediately under the shot (Fig. 19; line 16). Since this event rivalled the first arrival in amplitude, such a mechanism is clearly a potent source of second arrivals.

In deep water, where the water wave masked first arrivals from the sediments, lines of second events which corresponded in velocity and intercept times to refracted arrivals from sedimentary layers, could be picked within 20 km. of receiver positions. Much of the sedimentary section in the "Bransfield Trough" was established on the evidence of such arrivals.

The technique of firing shots by cable meant that shot density near the receiver was not sufficient to identify reliably any near-vertical reflections from within the sediments.

A representative set of two-ship records showing mantle arrivals appears in Fig. 5.

2. *Corrections to the data*

All times shown in the accompanying travel-time graphs have had the delay in the water layer subtracted as part of a correction which also incorporates the effect of varying shot depths. This correction takes the form:

$$\left\{(d_{ws}-d_s)+(d_{wr}-d_h)\right\}\frac{\cos(\sin^{-1} V_w/V_r)}{V_w},$$

where d_{ws} is depth of water at shot, d_{wr} is depth of water at receiver, d_s is depth of shot, d_h is depth of hydrophone, V_w is velocity of sound in water, and V_r is velocity of sound in refractor. Approximate refractor velocities obtained from uncorrected time–distance plots were used here.

In addition, a correction for variation in sea-bed topography was made on most lines. On lines 24 and 25, the method described by Officer and others (1959) was applied. However, where the structure of the shallow layers along the line was better established (e.g. where sonobuoy lines had been shot at points along the line), the effects of topography were incorporated in correcting the deep arrivals' times to a new datum level at about the base of the sediments by using the delay-time formula:

$$t_s = \frac{h_s \cos(\sin^{-1} V_s/V_r)}{V_s},$$

where t_s is the delay time through a thickness h_s of sediment of velocity V_s for arrivals from a refractor of velocity V_r. A new time–distance graph of deep arrivals was then drawn using these corrected times and the interpretation of the deeper layers was completed relative to the new datum.

In some cases, where the sea bed showed considerable topography, valuable information was obtained on the velocities of the rocks immediately beneath the sea bed by finding out which value of V_s in the topographic correction reduced scatter on the first arrivals from a deep refractor to a minimum (e.g. line 29; p. 27).

3. *Calculation of velocities and depths*

On account of the variety of the data, no uniform procedure of interpretation could be adopted on all lines. In general, it was assumed that layers of uniform velocity are separated by plane interfaces. On most lines, velocities were measured from straight lines fitted to the travel times by the method of least squares, but lines were fitted by eye where there were only five points or less and for most of the sonobuoy graphs. On most lines, arrivals from sedimentary layers occurred as second events on the records and they ceased to be reliably identified within 20 km. of the receiver, so that they remained unreversed. For this reason and also because of lateral velocity variations, the standard method of Ewing and others (1939) could not be applied for every layer. Instead, for each receiving point, depths in the sediments were calculated from

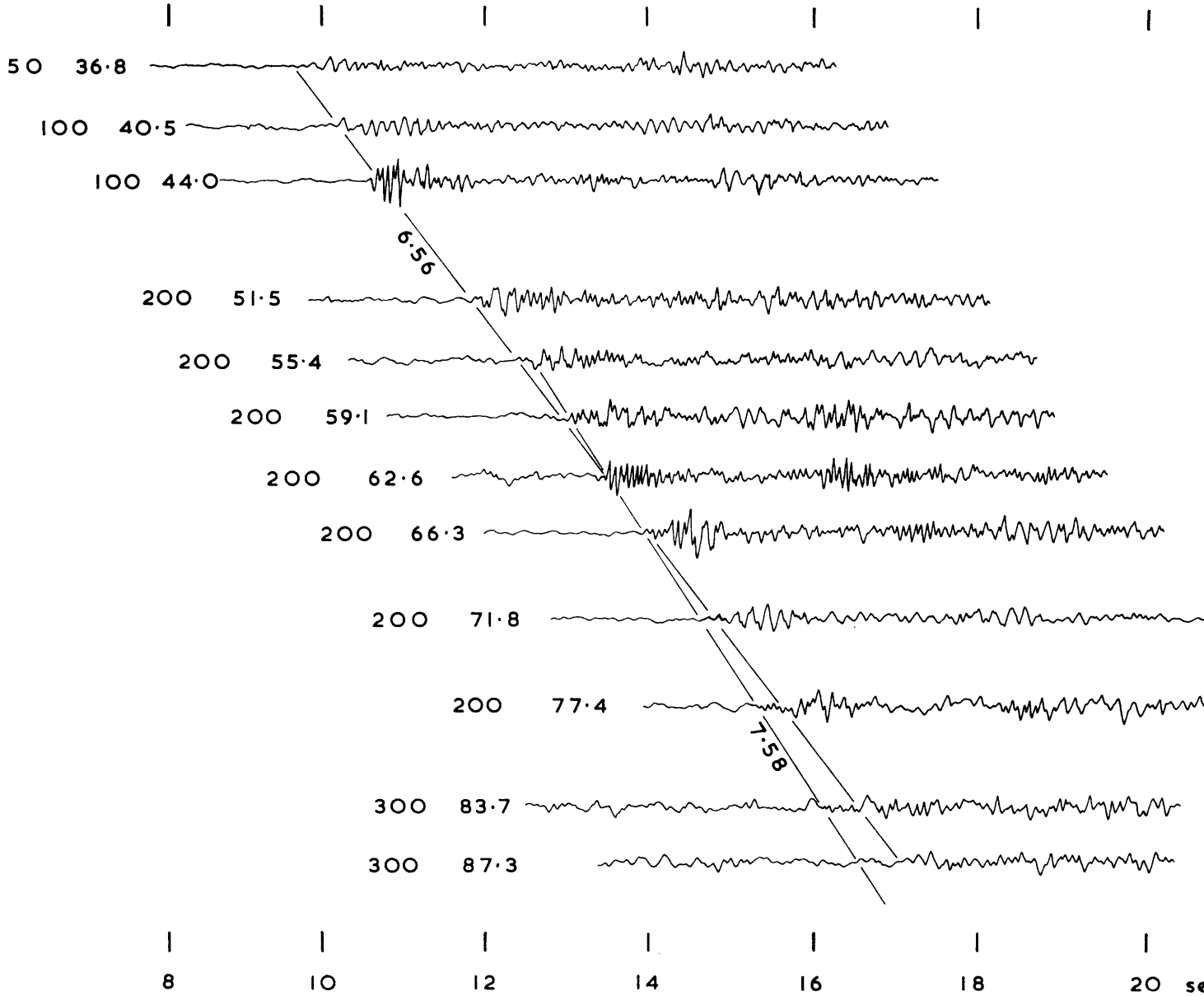

FIGURE 5

Two-ship seismic records; line 25 SW. The figures against each record refer to charge weight (lb. T.N.T.) and range (km.), respectively.

apparent velocities. Since the dip of the sediments is generally shallow (less than 5°), little error should arise from using apparent velocities. The dip is also low on the deeper refractors, often allowing calculation of refractor velocity simply from the arithmetic mean of apparent velocities in each direction. In the case of the land–sea lines, the velocities of sediments had to be assumed at times in order to make any interpretation at all. Also, on these lines the deeper refractors are often unreversed.

Depths were calculated by using the intercept-time relation for arrivals from the n^{th} layer of a series of horizontal layers:

$$T_n = 2 \sum_{k=1}^{n-1} \frac{h_k \cos i_k}{V_k},$$

where T_n is the intercept time for the n^{th} layer, h_k is the thickness of the k^{th} layer, V_k is the velocity of the

k^{th} layer, and $i_k = \sin^{-1}(V_k/V_n)$. This can be extended to gently dipping layers (dip $< 5°$) with negligible error.

On land–sea lines, delay-time calculations have been extensively used to delineate interfaces. The method depends on the general equation:

$$T = X/V_r + D_s + D_r,$$

where T is travel time, X is range, V_r is refractor velocity, D_s is delay time at shot, and D_r is delay time at receiver. Velocities and depths in all calculations have been taken to the second place of decimals to minimize rounding-off errors.

4. *Sound ranging*

No difficulty was experienced in recording the direct water-wave arrival in this area, since there is a positive velocity–depth gradient everywhere. Water-wave ray paths were investigated in some detail and it was found that, in water depths of not more than 1,800 m., the water-wave travel times could be represented by the equation $T = X/1{\cdot}450$ (T being travel time in sec., X range in km.), ranging errors being generally less than 0·1 km. and never greater than 0·2 km.

5. *Accuracy of the seismic results*

The results obtained from interpretation of the seismic observations are presented as a cross-section for each line showing the velocities and thicknesses of the various layers encountered. Errors in the velocities and depths may arise if there is deviation from the basic assumption of plane refractors of uniform velocity since this would lead to deviations of the arrival times from a straight line. In the present work the standard error obtained from the fitting of straight lines to the travel-time data by the method of least squares was generally $\pm 0{\cdot}05$ km./sec. for velocities and $\pm 0{\cdot}05$ sec. for intercept times on the two-ship lines, leading to errors in depth of the order of 5 per cent.

However, this is by no means an accurate estimate of the overall error in depth. An additional error is introduced by drift of the receiver and by the fact that the "shot boat" never follows exactly the same reciprocal course. Moreover, an error may be introduced where the thicknesses of the sedimentary layers are calculated from the intercept times of second arrivals. If the true beginnings of the wave trains cannot be distinguished from background noise, it may be that the events have been consistently picked late. The calculated depth of the interface within the sediments may thus be too great, leading to an error of about the same magnitude in the position of a deep refractor.

Perhaps the best way of estimating error in overall depth is by taking the observed mis-tie in depth of the deep layers where two lines cross and where the interpretations have been made independently. This is possible at two places—in the middle of Bransfield Strait (lines 32 and 25) and north-west of the South Shetland Islands (lines 26 and 27). The results are tabulated in Table I.

TABLE I

ERROR IN DEPTHS TO SEISMIC INTERFACES AT THE INTERSECTION OF LINES

Lines	*Refractor velocity* (km./sec.)	*Mean depth* (km.)	*Percentage difference from the mean*
26 and 27	5·92–6·03	6·31	7
	6·67–6·70	10·20	4
32 and 25	5·30	4·25	9
	6·49–6·60	5·32	3

From the above discussion it would appear that a reasonable estimate of the percentage error in depth is 10 per cent. It should be noted that this applies to the better data in the area—the two-ship and sonobuoy lines. When gross assumptions have to be made about the sedimentary layers, as in the interpretation of certain land–sea lines, or the data are sparse, as in the case of mantle arrivals, uncertainties are correspondingly increased.

VI. RESULTS OF THE SEISMIC SURVEY

THE seismic data fall conveniently into four groups of lines. Within each group a coherent interpretation can be made which outlines the structure of a particular area. For each line a travel-time graph and depth section is shown and the results are summarized in four geological cross-sections shown in Figs. 31–34. Since methods of interpretation varied so much from one line to another, a brief review of the results of the four groups of lines is given below.

In the following account and in Fig. 1 the notation "line 18NW", etc. should be interpreted as "line 18 shot towards the north-west". In the sections accompanying each line, solid lines represent interfaces for which there is some direct seismic evidence, broken lines indicate interfaces for which there is no direct evidence and assumed values of velocity are indicated in brackets.

1. *Mid-Bransfield Strait* (lines 18, 20, 24, 25, 31 and 32)

a. *Lines 24, 25 and 31.* Lines 24 and 25 are reversed two-ship lines shot parallel to the Scotia arc in order to obtain a good crustal section in the middle of Bransfield Strait and thus supplement the data of previous land–sea lines 18 and 20. Somewhat later, sonobuoy line 31NE was shot from a single buoy laid in the middle of line 24.

Time–distance graphs and depth sections are shown in Figs. 6 and 7. A topographic correction has been made at 4·0 km./sec. to datum levels 1·64 and 1·95 km. below sea-level, on lines 24 and 25, respectively.

In both lines the sedimentary sections are entirely dependent on second arrivals and the majority of first arrivals, showing apparent velocities of about 6·5–6·6 km./sec., are from the main layer of the crust. In line 24, deviations of arrival times from a straight line occur in both directions of shooting in such a way as to indicate topography on the refractor surface. For the purpose of calculating the best-fitting straight line to the arrivals, these points on line 24 have been omitted. Line 31 is useful in confirming the shape of the travel-time graph here.

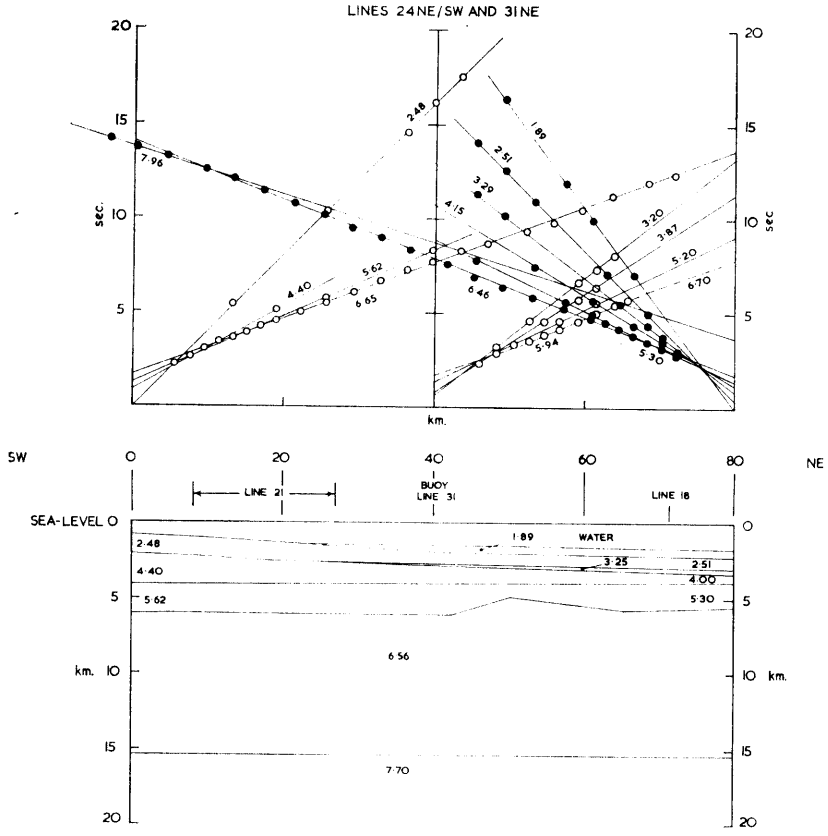

FIGURE 6

Time–distance graph and section; line 24 NE/SW and sonobuoy line 31 NE.

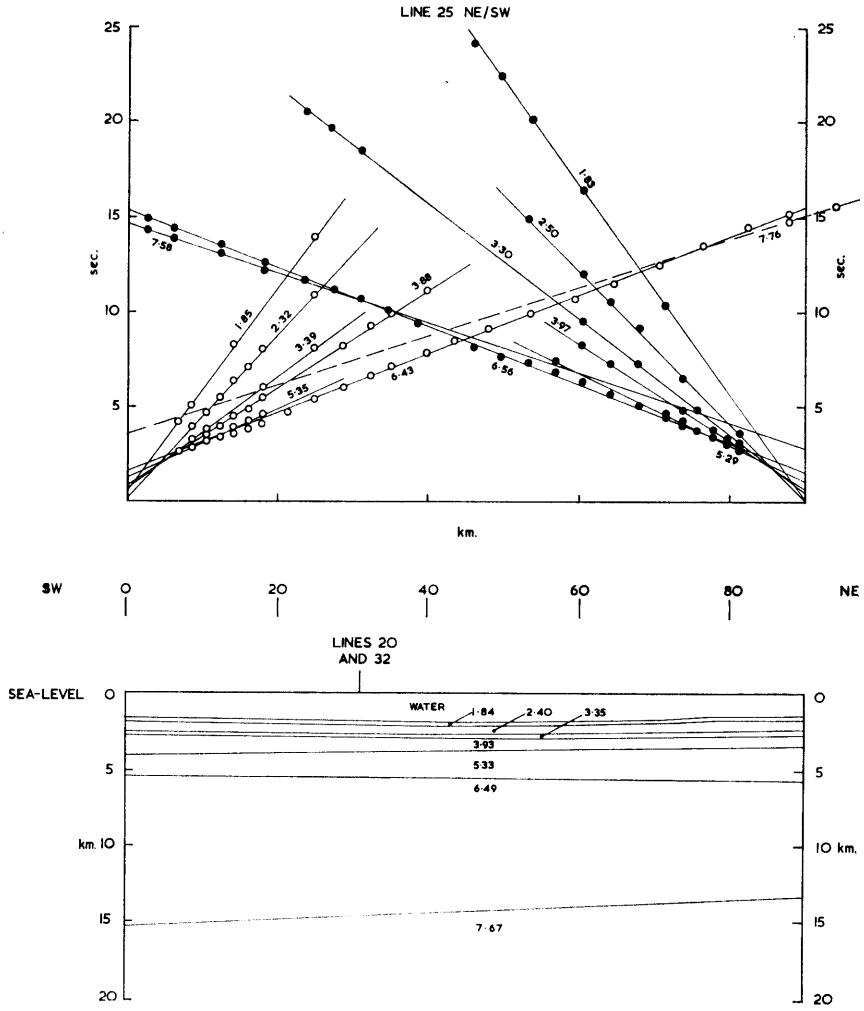

FIGURE 7

Time–distance graph and section; line 25 NE/SW.

On line 25, deviations from straight lines do not correspond in each direction of shooting and they cannot be explained by topography on the refractor surface. They may be due to variations in the near-surface layers arising from a difference in the course steamed by H.M.S. *Protector* during each shooting run. Considerable deviation in the range 12–18 km. (shooting north-east) may be due to a thin, impersistent high-velocity layer (about 7·0 km./sec.) and these points have been excluded in calculating the best straight line of velocity 6·43 km./sec.

On both lines the most distant arrivals shooting to the south-west fall on alignments of distinctly higher velocity, 7·96 and 7·58 km./sec. Unfortunately, this layer is not well reversed but on line 25NE arrivals on the last two shots permit a tentative line to be drawn matching the intercept time at the junction of the lines with that for line 24SW and giving an apparent velocity of 7·76 km./sec. From this the section in Figs. 6 and 7 follows.

Although the evidence for the deepest layer is not conclusive by itself, there is further support from the other lines in this group reviewed below (p. 14-15).

b. *Sonobuoy, line 32.* This sonobuoy line was shot along part of line 20, an earlier land–sea line, in order to provide data on the crustal structure under the deep water of the "Bransfield Trough" and thus enable a more complete interpretation of the earlier results.

Four buoys were laid in the middle of Bransfield Strait and a line of shots fired north-westwards into Admiralty Bay, King George Island (Fig. 1). The time–distance data, corrected for topographic variations at 2·7 km./sec. to a datum 1·9 km. below sea-level, are shown in Fig. 8, where each buoy has been considered

as a separate receiver. The alternative presentation, a range plot using the four buoys as a multiple detecting unit, was possible only for a few shots, since one of the buoys failed to function properly. A range plot for two such shots is shown in Fig. 9.

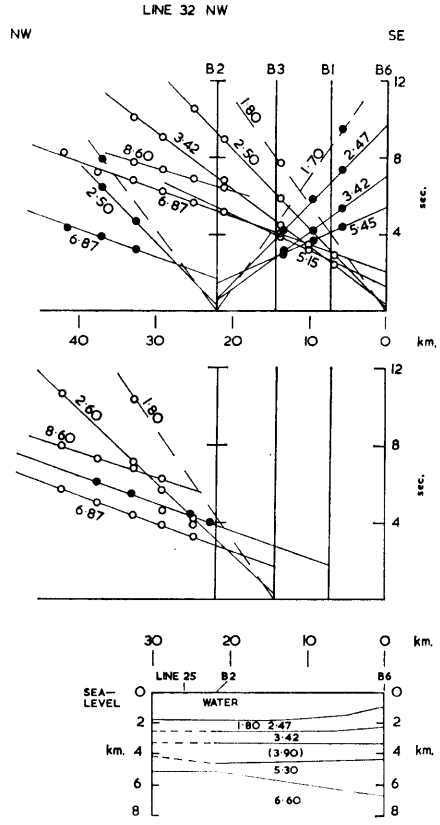

FIGURE 8

Time–distance graphs and section; sonobuoy line 32 NW. B2, etc. refer to sonobuoy positions. Each buoy has been treated as a separate receiving point. Additional first arrivals from shots farther to the north-west are shown in Fig. 10.

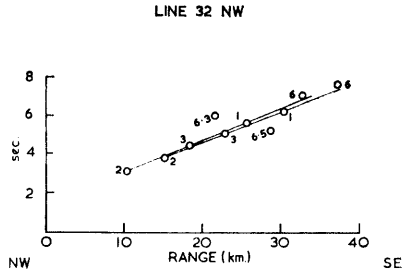

FIGURE 9

Time–range graph for two shots; line 32 NW. Numbers against travel times refer to the sonobuoy which recorded the seismic arrival.

Some interesting evidence on the velocity of the shallow layers is provided by this range plot. The south-easternmost buoy (6) was positioned at the top of the slope forming the south side of the "Bransfield Trough"; in order to bring the arrival times for this buoy into alignment with the others, a topographic correction must be made. It can be shown that the topographic correction velocity cannot be greater than 2·7 km./sec., i.e. that the slope is underlain by sediment (Fig. 8).

On the time–distance graph itself, sedimentary layers are represented only by second arrivals at about 2·5 and 3·4 km./sec. The layer at 3·9 km./sec. shown in Fig. 8 has been assumed to be present by analogy with line 25, which this line intersects.

The main crustal layer (velocity 6·6 km./sec.) is represented by first arrivals of apparent velocity 6·87 km./sec. and, on the range plot, 6·40 km./sec. The refractor velocity (6·6 km./sec.) and its depth (5·2 km.) compare well with those obtained on line 25 nearby.

In Fig. 8 there is a persistent line of second arrivals with an apparent velocity of 8·6 km./sec. These occur at the correct range to be wide-angle reflections or refractions at near the critical angle from the deepest layer detected in the area (7·6 km./sec.), which dips gently south-eastwards here. First arrivals with a similar apparent velocity were recorded on land–sea lines 18 and 20, shooting north-west (Figs. 10 and 11).

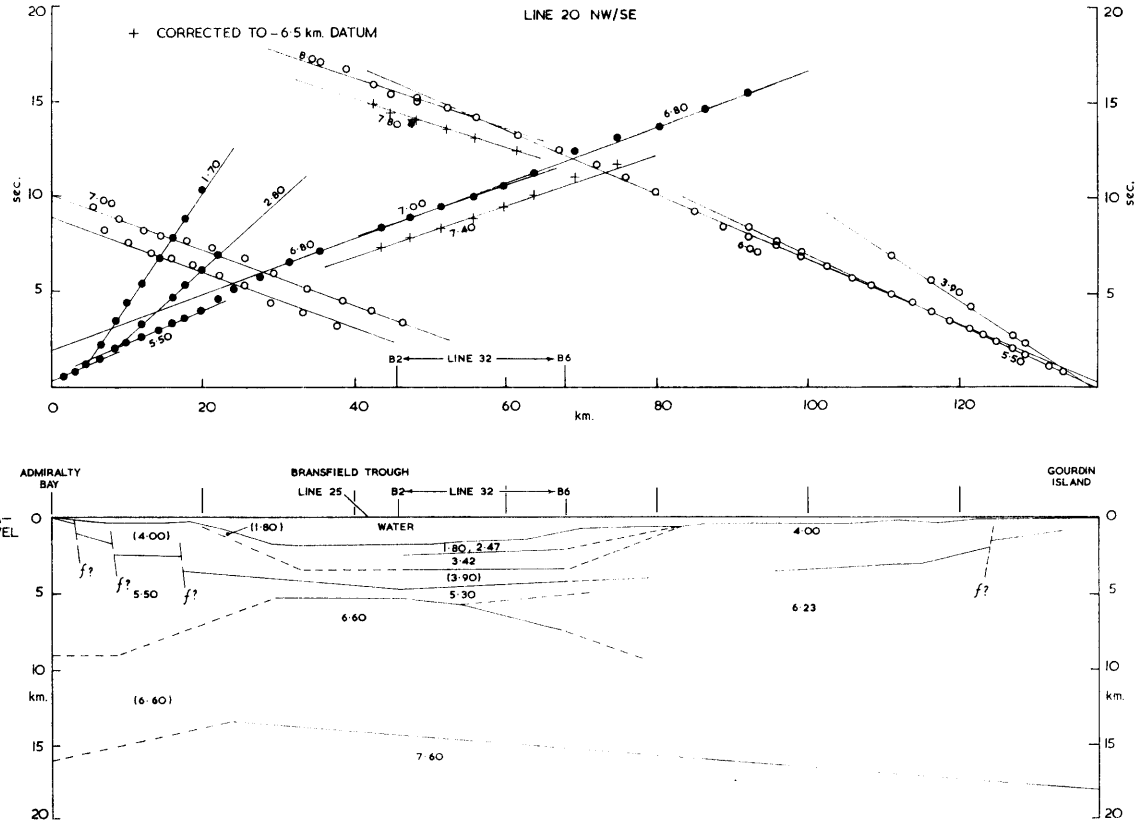

FIGURE 10

Time–distance graph and section; line 20 NW/SE. The sonobuoy positions for line 32 and distant shots on that line are also shown; the section derived from line 32 has been incorporated *en bloc* in that for line 20 NW/SE.

c. *Land–sea lines 18 and 20.* Time–distance graphs and appropriate sections for these lines are given in Figs. 10 and 11. Times are corrected only for delay in the water layer. Like all land–sea lines, additional information is required about the structure of the shallow layers in the middle of the line before a satisfactory interpretation can be made, and this is provided by lines 24, 25, 31 and 32 which are reviewed above.

On both lines the early shots at the north-west end, off the South Shetland Islands, show alignments of about 5·5 km./sec. These may be arrivals from Jurassic volcanic rocks which are known to underlie the Tertiary lavas forming most of the exposures. Geological investigations have shown large normal faults parallel to the coast with downthrows to the south-east (Barton, 1965), and these are presumed to be the cause of the observed steps in the line of first arrivals. Second arrivals on line 20 show sedimentary alignments of 1·70 and 2·80 km./sec., but these are taken to have a negligible thickness along the bottom of the bay and 4·0 km./sec. has been assumed as the velocity of the Tertiary volcanic rocks—a value chosen from results around Deception Island and the evidence obtained by Raitt (1957) on Eniwetok atoll.

At the south-eastern end of both lines there is little doubt on bathymetric grounds that the sea bed, for some considerable way off the coast of Trinity Peninsula, is rocky in nature (p. 4), and in Fig. 10 the thick sediments under the southern edge of the "Bransfield Trough" have been drawn as thinning arbitrarily towards the coast. Immediately off the coast of the peninsula on line 20, the 5·5 km./sec. alignment is

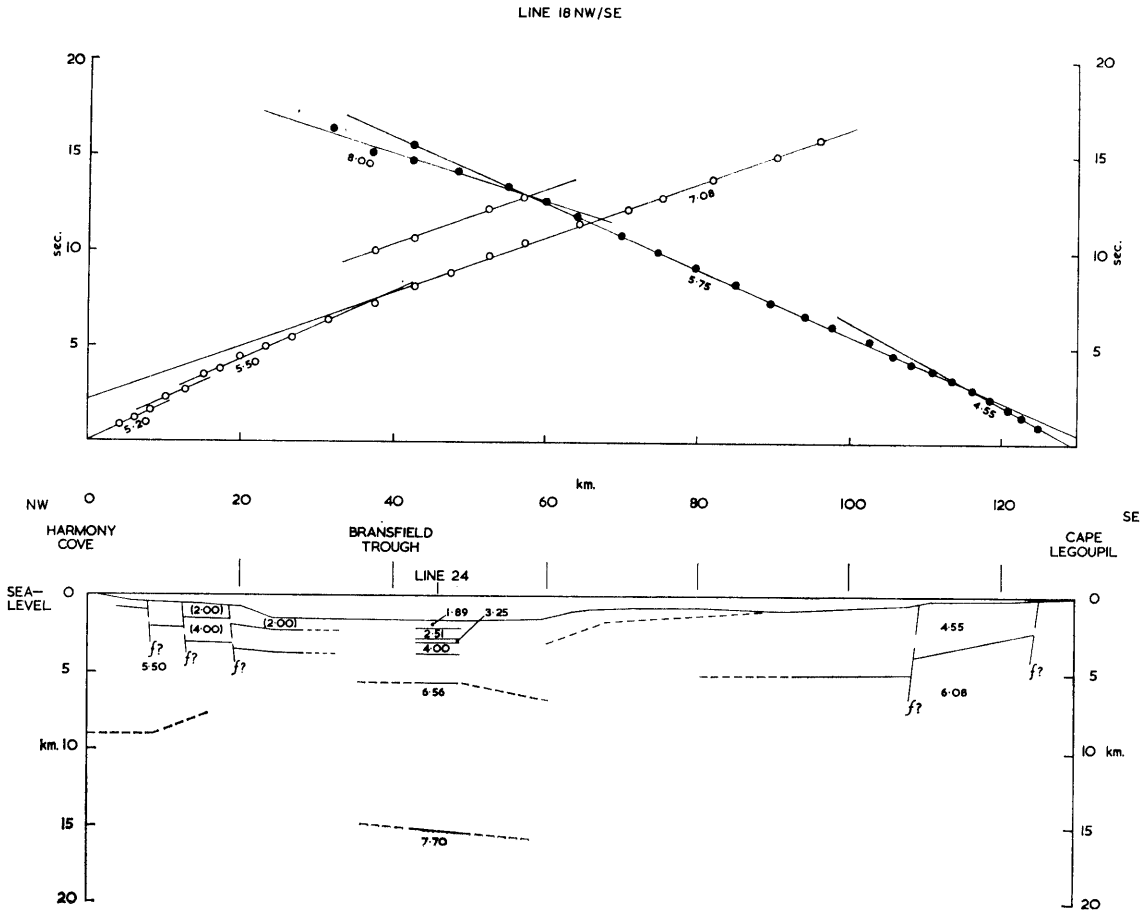

FIGURE 11

Time–distance graph and section; line 18 NW/SE.

taken to arise from the metasediments and plutonic intrusions known to crop out on Trinity Peninsula, while second arrivals showing 3·9 km./sec. may represent sediments or volcanic rocks downfaulted off the coast in the same way as they occur farther south-west at Cape Legoupil (Halpern, 1964). There they give rise to first arrivals on line 18NW with an apparent velocity of 4·55 km./sec. (Fig. 11).

In the middle of the section for line 20, the structure for the middle of Bransfield Strait deduced from line 32 has been placed in its appropriate position. It should be noted how the travel times from the land–sea shots confirm the presence of thick sediments under buoy 6 (line 32) by showing an appropriate delay (e.g. Fig. 10, shots at 69 and 75 km.).

Turning to the deeper layers, the long line of first arrivals of apparent velocity 5·75 and 6·00 km./sec., shooting north-west on both lines, must represent continental crustal rock extending out from the coast of Trinity Peninsula. By using the known delay through the sedimentary section in the vicinity of lines 24 and 25 in the middle of the strait and the observed travel times, an overall velocity for this crustal rock was calculated to be 6·08 km./sec. on line 18 and 6·23 km./sec. on line 20. It should be noted that the results from the lines in the middle of Bransfield Strait are clear enough to indicate that such crustal rock is very thin there, and it is presumed to grade into the 6·60 km./sec. layer or perhaps pinch out in the manner shown in Fig. 10.

It is convenient now to consider the question of the deepest refractor (velocity about 7·7 km./sec.) mentioned in connection with lines 24, 25 and 32. Further evidence for this refractor, derived from the land–sea lines, may be summarized as follows:

i. On line 20SE, travel times across the position of the buoy spread of line 32 show an apparent velocity of 7·0 km./sec. But on line 32 the 6·6 km./sec. layer gave an apparent inter-buoy velocity

of 6·4 km./sec. across the same position, so that the arrivals on line 20 must refer to a deeper layer of higher velocity.

ii. The distant shots of sonobuoy line 32 laid in Admiralty Bay corroborate the apparent velocity on the land–sea line, since they show an apparent velocity of $7 \cdot 10 \pm 0 \cdot 14$ km./sec. across the buoy spread.

iii. In the reverse direction, on both lines 18NW and 20NW, the last few points fall on a poorly defined alignment of apparent velocity approximately 8·0 km./sec. (Figs. 10 and 11).

iv. When corrected to a datum 6·5 km. below sea-level, the reversed arrivals on line 20 give a true refractor velocity of $7 \cdot 6 \pm 0 \cdot 15$ km./sec. (Fig. 10).

v. If the refractor depth is taken as 14 km. (from line 25) and its velocity as 7·6 km./sec., travel times calculated on the basis of the section shown in Fig. 10 fit the observed times on the land–sea line.

For this purpose it is necessary to assume a structure under one end of line 20, and in Fig. 10 the interface shown has been constructed to fit the observed gravity gradient along Admiralty Bay as depicted by Griffiths and others (1964). The depth of this layer beneath Trinity Peninsula is also doubtful and indeed its very existence there is problematical in view of the heterogeneity of material likely to be encountered under this Tertiary fold belt. However, the present time–distance data indicate a minimum thickness of 18 km. of rock at about 6·2 km./sec. under the coast of the peninsula.

2. *The vicinity of Deception Island* (lines 16, 17, 21, 22 and 30)

It is evident from Fig. 1 that Deception Island was used as the receiving point for several land–sea lines and these may conveniently be considered together. The island, which takes the curious form of a broken ring enclosing the anchorage of Port Foster (Fig. 12), has been built by successive volcanic eruptions from a variety of vents from (?) Tertiary to Recent times with intervening periods of subsidence (Hawkes, 1961*b*).

a. *Line 30.* As a key point in the land–sea seismic work, an attempt was made to investigate the structure of Deception Island itself by means of a short sonobuoy line shot across Port Foster (Fig. 12).

Travel times corrected for delay in the water layer are shown in Figs. 13 and 14 separately for each buoy, and as a range plot in Fig. 15. The most straightforward interpretation of these plots is shown in the section in Fig. 16, and rather surprisingly, no faulting is evident. Large arcuate faults can be seen to have

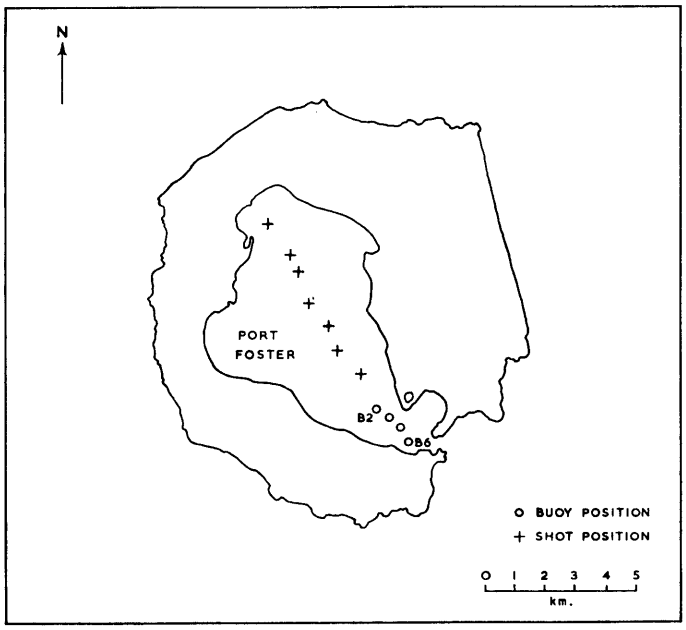

FIGURE 12

Location of sonobuoy line 30 NW/SE; Deception Island. B2 and B6 refer to individual sonobuoys for which time–distance data are shown in Figs. 13 and 14.

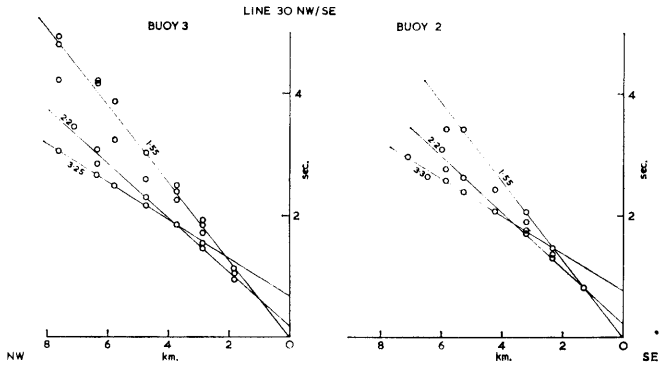

FIGURE 13
Time–distance graph for sonobuoys 3 and 2; line 30 NW/SE; Deception Island.

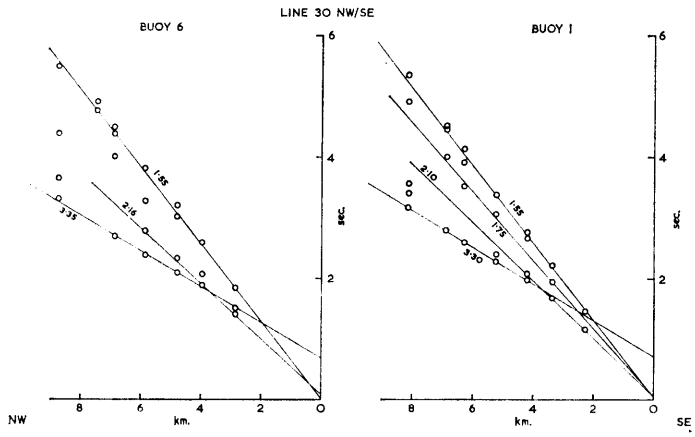

FIGURE 14
Time–distance graph for sonobuoys 6 and 1; line 30 NW/SE; Deception Island.

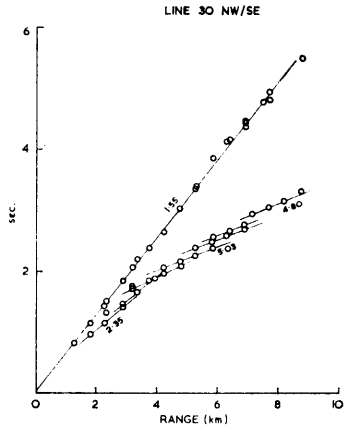

FIGURE 15
Time–range graph for all four sonobuoys; line 30 NW/SE; Deception Island.

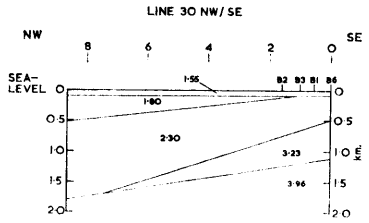

FIGURE 16

Section for line 30 NW/SE; Deception Island.

formed conspicuous scarps in the hills surrounding Port Foster (Hawkes, 1961*b*) and the present results suggest that these were more important than radial faults, so that the middle of the island seems to have subsided more or less *en bloc*.

Taken in conjunction with the known geology, the velocities of the layers suggest that they are of ash and assorted volcanic debris in various degrees of compaction. The velocity of the deepest layer (3·96 km./sec.) is similar to that found in the upper layers of atolls and guyots where dredging has shown volcanic rocks, not reef limestones, forming the bedrock. The thick layers at the comparatively low velocities of 1·8 and 2·3 km./sec. are to be expected, if only from the large amounts of ash being brought down at the present time by glaciers and melt-water streams.

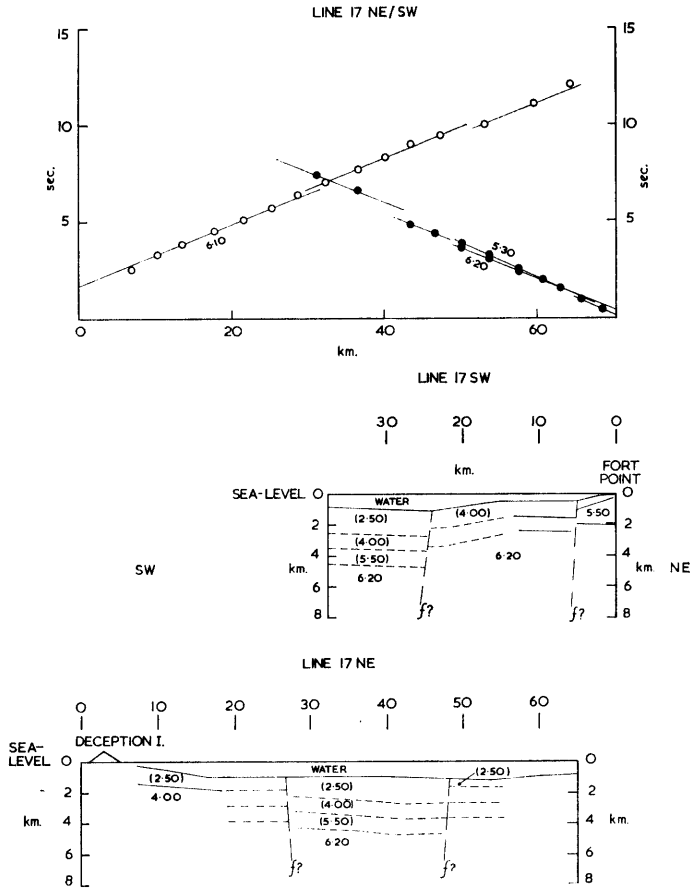

FIGURE 17

Time–distance graph and sections; line 17 NE/SW. Assumed values of velocity and thickness have had to be used for the shallow layers.

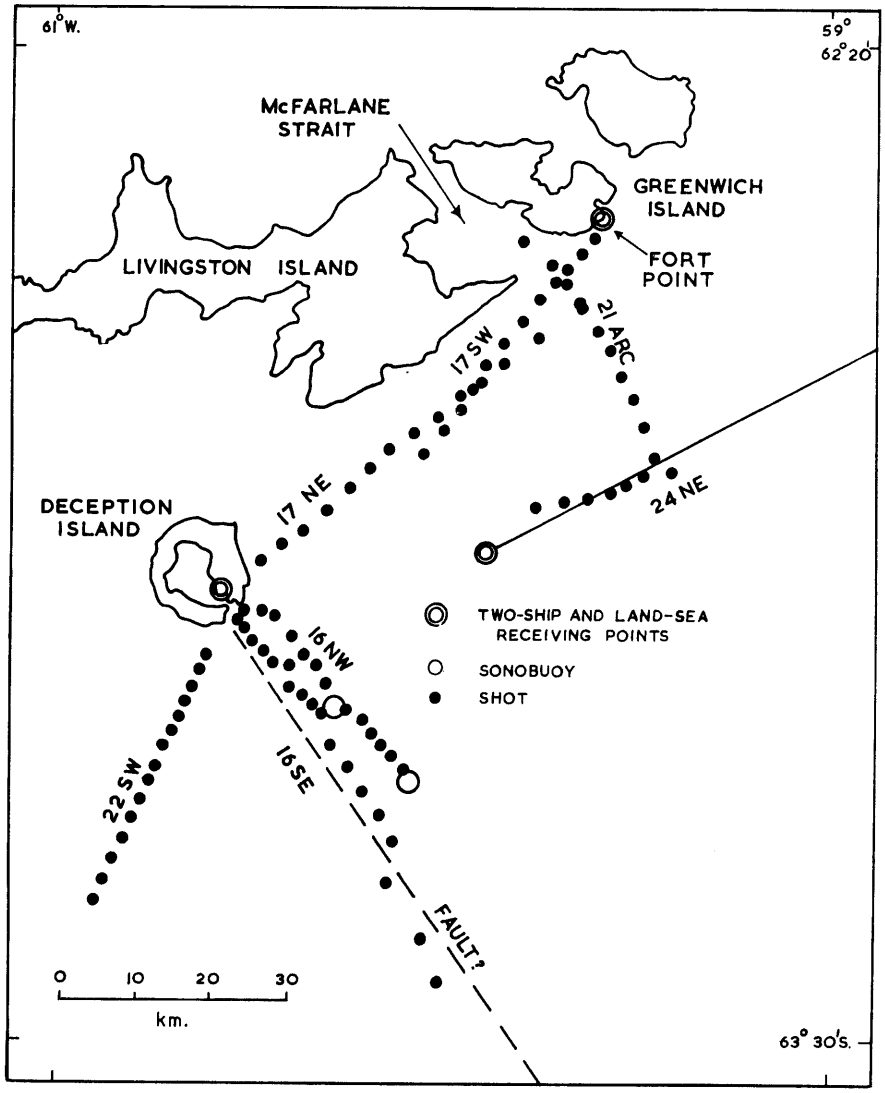

FIGURE 18

Map showing details of seismic lines in the vicinity of Deception Island.

b. *Line 17.* The time–distance graph and sections for this line are given in Fig. 17. Times are corrected for water delay only and, in view of the difference in position of the two lines of shots (Fig. 18) and the amount of extrapolation, no reciprocal time tie is indicated. Where the lines overlap, the first arrivals have approximately the same slope of about 6·2 km./sec. in both directions of shooting; the most straightforward interpretation of the alignments is that a nearly flat refractor has been faulted up to the north-east, causing the large time steps seen on both lines.

There is no information on the velocities and depths of the shallow layers away from the islands and the layering shown in Fig. 17 (1·0 km. at 4·0 km./sec. and 1·0 km. at 5·5 km./sec.) has been assumed by analogy with the results of lines 24 and 16 in the same vicinity. Time variations on the 6·20 km./sec. alignment are then treated as thickness variations in a layer of velocity 2·5 km./sec.

It is evident that the line confirms the presence of faulting along the south-east coast of Livingston Island, but perhaps the most surprising feature to emerge is the relatively low velocity (6·2 km./sec.) of the main crustal layer between Deception and Livingston Islands; this topic is discussed further in the consideration of line 21 (p. 21).

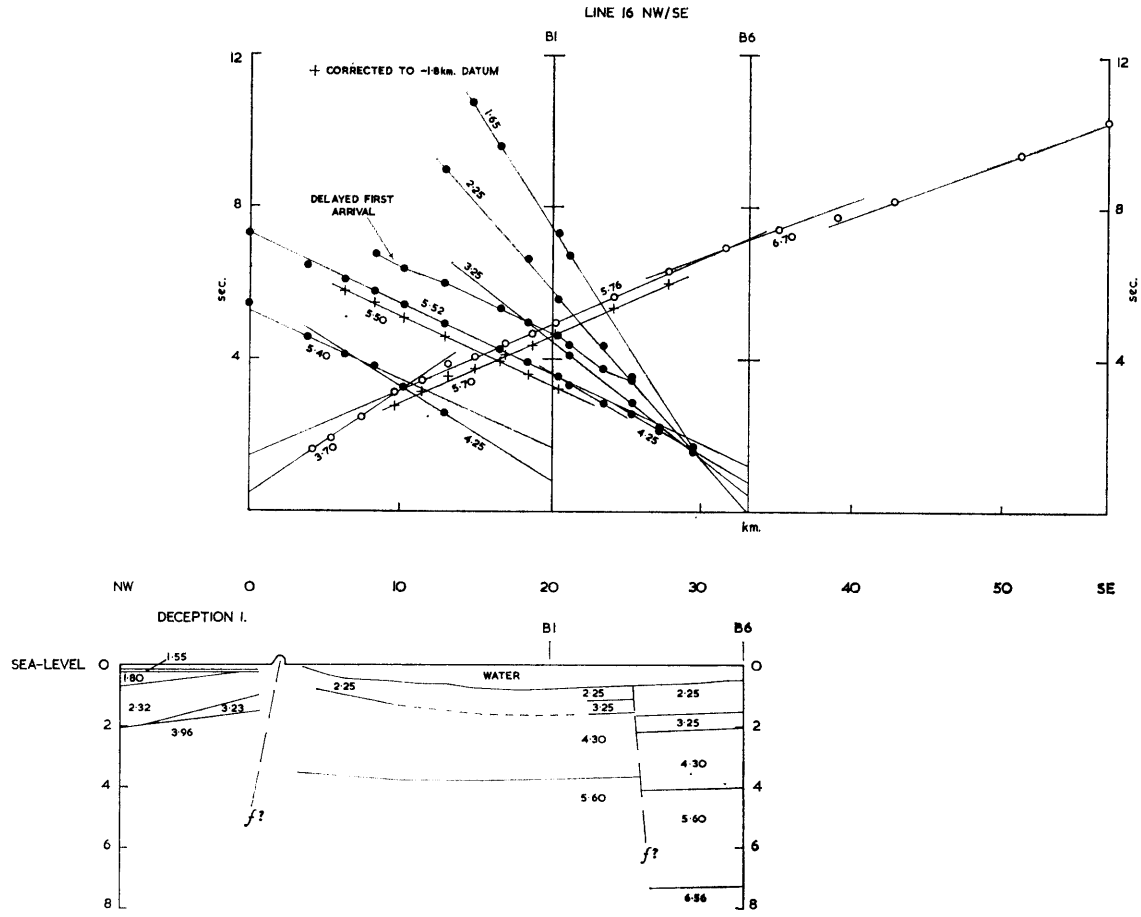

FIGURE 19

Time–distance graph and section; line 16 NW/SE. B1 and B6 refer to sonobuoy receivers. A delayed first arrival arising from reflection once in the water layer under the shots is shown. The section under Deception Island obtained from line 30 is also incorporated.

c. *Line 16.* Although it is treated as a reversed line, this comprises two lines shot in different circumstances and at different times. Line 16SE is an early land–sea line, while 16NW is a sonobuoy line shot as a reversal of the land–sea line at a later date, using two moored buoys as receivers (Figs. 1 and 18).

The time–distance plot (Fig. 19) shows a good tie in reciprocal times of the first arrivals and enough second arrivals from the sonobuoy shots to give the necessary shallow section away from Deception Island. Apparent velocities have been used in calculating this section. For convenience, the section inside Deception Island (derived from line 30) has also been shown here.

The velocity of the 5·6 km./sec. layer was found by correcting the first arrivals down to a datum 1·8 km. below sea-level (Fig. 19). The position of this layer was then calculated from the arrivals on line 16SE using a delay time at Deception Island of 0·73 sec., determined from the mean overall travel time and the known intercept time at buoy 6.

The most distant shots show an apparent velocity of 6·70 km./sec. with a marked discontinuity. There can be little doubt that the refractor commonly seen on the lines in mid-Bransfield Strait with velocities in the range 6·5–6·6 km./sec. is also present here, and its position has been calculated in the section using a delay time at Deception Island of 0·91 sec. and an overall refractor velocity of 6·49 km./sec. as found on line 21 (p. 21). The discontinuity in the alignment will be discussed more fully in connection with line 22 (p. 21).

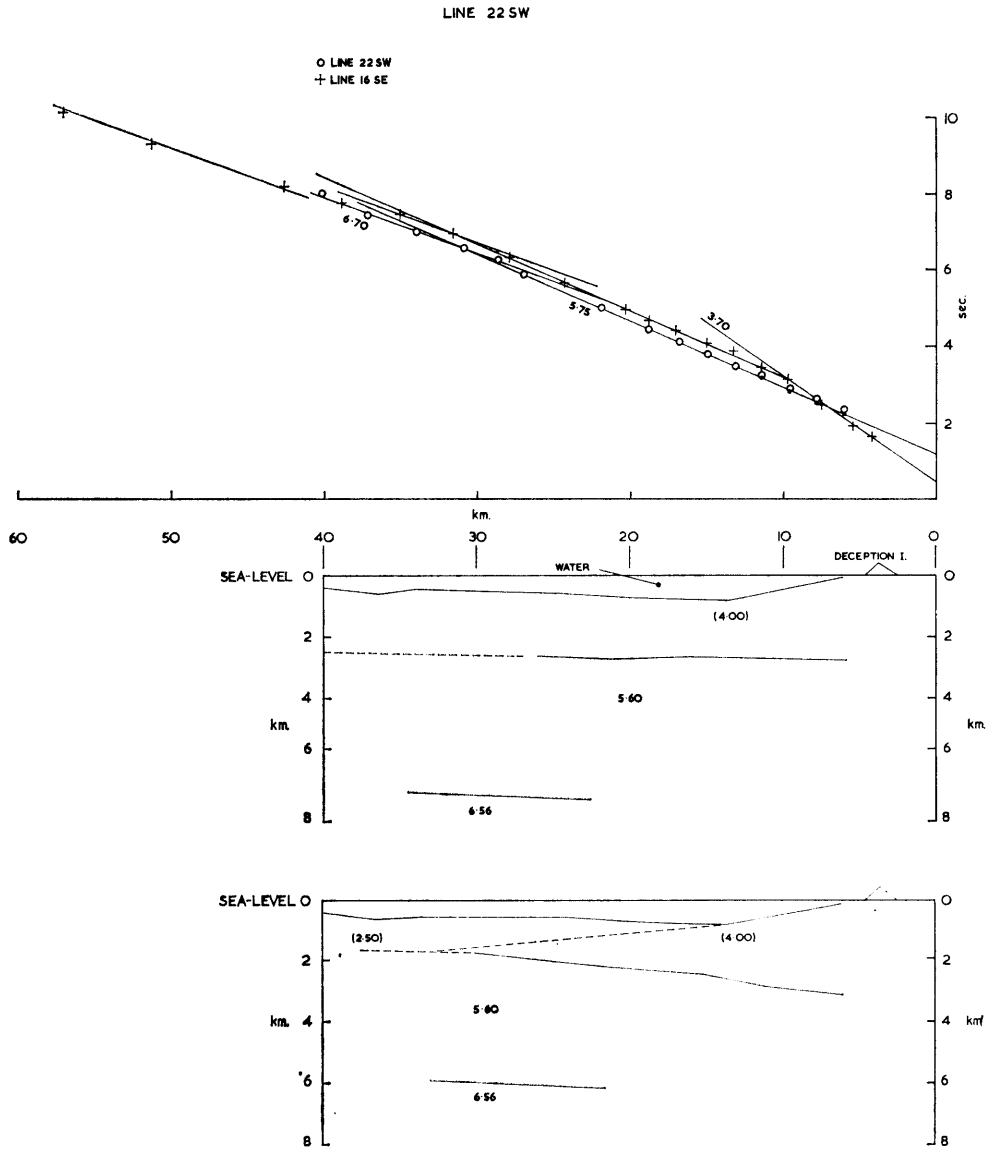

FIGURE 20

Time–distance graph and section; line 22 SW. First arrivals from line 16 SE are also shown for comparison.

No attempt has been made to indicate the structure at depth beneath Deception Island, because there is no information on the velocities of the rocks below the 4·0 km./sec. layer. However, the depth of the 6·2 km./sec. layer cannot be greater than that of the 6·6 km./sec. layer outside the island, so that the structure of the island would seem to consist of a pile of lavas built up on top of a largely level crust.

d. *Line 22.* This early land–sea line is not supported by any sonobuoy work. The time–distance plot is shown in Fig. 20 with that of line 16SE for comparison. It is clear that apparent velocities on the two lines are very similar, but times on this line are all about 0·3 sec. less than on line 16SE.

There are two possible explanations for this:

i. Delay time to the 5·6 km./sec. layer at Deception Island has decreased by 0·3 sec. relative to line 16 (because the lines were shot in different directions).

ii. The shallow-layer structure is considerably different from that of line 16.

Since the total delay time at Deception Island is, in any case, only 0·73 sec., the second alternative is adopted here and Fig. 20 shows two limiting cases of the shallow-layer structure. If the section showing

sediments at 2·5 km./sec. is taken as being the more likely, the 5·6 km./sec. layer has been upfaulted 2 km. relative to line 16.

The possibility of a fault between these two lines suggests an explanation for the displacement seen on the most distant arrivals of line 16SE of apparent velocity 6·70 km./sec. It should be noted that these are so displaced as to coincide in time with the most distant shots on line 22 (Fig. 20). From Fig. 18 it will be seen that the last three shots on line 16 are offset to the south-west from the rest of the line and they may lie across the fault postulated as separating these lines, and on its upthrown side. If this were so, a step would appear on the time–distance graph in the manner observed. It is on this evidence that a fault has been drawn across Bransfield Strait in Fig. 2.

Before concluding discussion on line 22, it should be observed that the early first arrivals, from points on the submarine slope of the island, fall exactly on the line of the majority of first arrivals when corrected for the topographic rise of the islands using a velocity of 4·0 km./sec. Thus they provide indirect evidence that the pile of lavas forming Deception Island has approximately this same velocity.

e. *Line 21.* This land–sea line was shot from Deception Island into Bransfield Strait to investigate possible faulting along the south-eastern side of the South Shetland Islands. From Fig. 18 it can be seen that shots were first laid in a straight line from Deception Island towards the north-east over a suitable range to confirm that the required refractor was being followed and then brought approximately in an arc into McFarlane Strait. Two-ship line 24 was later positioned to coincide with the in-line section of line 21, so that the shallow structure deduced from the two-ship line could be used to supplement the land–sea line.

Travel times for the in-line section were corrected in the same way as for line 24 and they gave an apparent velocity of $6{\cdot}32 \pm 0{\cdot}17$ km./sec. The size of the error in this determination, compared with the error of $\pm 0{\cdot}05$ sec. usually found in the two-ship velocity alignments, is a measure of the poor quality of the data due to uncertainties in range. Over the same position, two-ship line 24 showed an apparent velocity of $6{\cdot}65 \pm 0{\cdot}04$ km./sec. and, although the value obtained from line 21 is smaller, there can be little doubt that it refers to the same refractor of true velocity 6·56 km./sec.

This line clarified several points in connection with the structure of the crust around Deception Island. From a knowledge of the shallow section at the mouth of McFarlane Strait and the travel times of the shots of line 21 (arc) at that point, a delay time to the top of the 6·2 km./sec. layer at Deception Island can be calculated (0·91 sec.); this was used in completing sections on lines 16, 17 and 22.

The second point concerns the areal extent of the 6·2 km./sec. crust found from the results of line 17 to underlie Deception Island. This extends north from Deception Island along the coasts of Livingston and Greenwich Islands, and it would probably be safe to predict that it underlies all the shallow water between Deception, Snow and Livingston Islands. However, lines 16, 22 and 24 show a velocity layering of the type 5·6/6·6 km./sec. under the deep water east, south-east and south-west of Deception Island, and the question arises as to how far the 6·2 km./sec. material extends in this direction.

Working from travel times for the in-line part of line 21 and the known delay at that point to the 6·56 km./sec. layer found on line 24, the mean overall velocity for the in-line shots can be calculated as 6·49 km./sec. This is less than the true velocity of the main crustal layer (6·56 km./sec.), because part of the travel path was in the 6·2 km./sec. rock immediately around Deception Island; it can be shown that, for an average path length of 50 km., approximately 10 km. of path must lie in the 6·2 km./sec. material. Therefore, this suggests that the 6·2 km./sec. layer extends no farther to the south and south-east than approximately the extent of the submarine slope around the island.

Finally, the arc part of line 21 may indicate where the 6·2–6·6 km./sec. lateral velocity change takes place off the entrance to McFarlane Strait. Delay times were calculated for the arc shots and they are given in Fig. 21. Since the refractor velocity used in the calculation was constant over the southern shots of the arc, any decrease in refractor velocity as the coast is approached should show as a decrease in delay time. However, no such decrease can be seen and it is inferred that the transition is abrupt and takes place under the steep slope leading up to the islands. In fact, there appears to be a small but systematic increase in delay time as the coast is approached, and this could possibly be due to a slight thickening of sediments.

3. *Shelf area north-west of the South Shetland Islands*

To investigate crustal structure under the South Shetland Islands, a pair of two-ship lines (26 and 27) was shot parallel to the arc as near the north-west coast of the islands as possible (Fig. 1), so that the

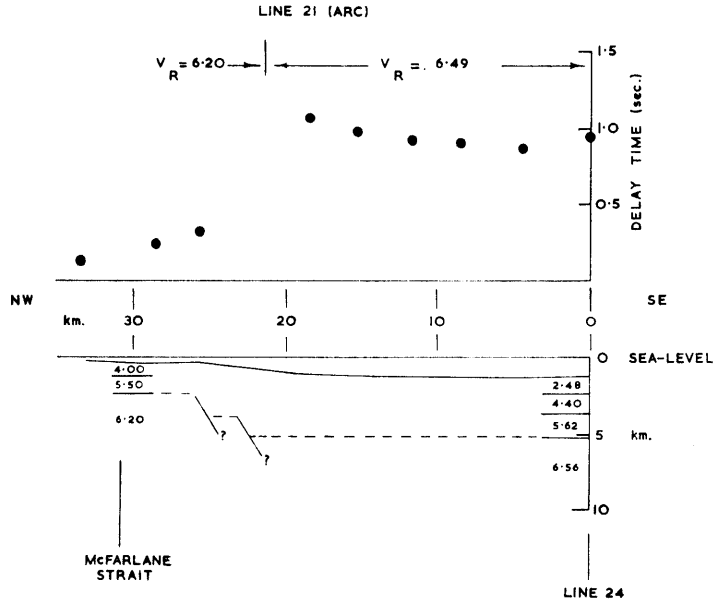

FIGURE 21

A plot of delay times to the 6·6 km./sec. layer calculated at the shot positions of line 21 (arc). The transition from the 6·6 km./sec. layer to rock at 6·2 km./sec. seems to be abrupt and sections from lines 24 NE/SW and 17 SW have been inserted to suggest the structure.

crustal section would be fairly representative of the block as a whole. Because of the shallowness of the water, the lines had to be shot farther offshore than was desirable and it is not certain how representative the results are of conditions under the islands themselves.

Sonobuoy lines 33 to 36 were shot later in the same position in order to gain more information about the shallow layers. The shooting technique consisted of mooring three buoys in line about 20 km. apart to act as receivers for shots dropped between them. Shots were graduated in size and two separate sets were dropped on each line to obtain reversal.

On both of the two-ship lines the interpretational approach has been, first, to obtain as good a profile as possible of the shallow layers along the line, then to correct the travel times of deeper layers to a new datum level within this section, and, finally, to calculate the velocities and depths of the deeper layers with respect to this new datum.

a. *Sonobuoy lines 35 and 36; two-ship line 26.* Travel times for the sonobuoy lines shown in Fig. 22 are corrected to a datum 0·46 km. below sea-level. The 1·90 km./sec. layer has appreciable thickness on these lines but the layer giving arrivals in the range 1·6–1·7 km./sec. is assumed to be of negligible thickness. In general, the velocities correspond well with those found at the ends of two-ship line 26 (Fig. 23).

On the travel-time graph for line 26 it can be seen that distant shots fall on to three different velocity alignments at approximately 5·75, 6·5–6·9 and 8·5 km./sec., interpreted as three different refractors. The tie-in reciprocal time on the 6·53–6·94 km./sec. alignment is good (to 0·1 sec.), indicating that the 8·53 km./sec. arrivals are from a different refractor. However, no corresponding set of arrivals can be seen in the reverse direction. If an alignment of approximately 8·0 km./sec. were fitted to the last two points shooting north-east, reciprocal times would disagree by only 0·2 sec. Since arrivals shooting south-west are beyond reasonable doubt, the alignment is assumed here to represent a separate refractor.

In constructing the section shown in Fig. 23 the sections from lines 35 and 36 were inserted *en bloc*, a new datum was established at the base of the sediments, i.e. at a depth of 4·5 km. below sea-level, and times for the deeper refractors were corrected to this datum. The new travel times are also shown in Fig. 23 and the velocities of the layers deduced from them (5·92 and 6·70 km./sec.) compare well with those found on line 27 (6·03 and 6·67 km./sec.).

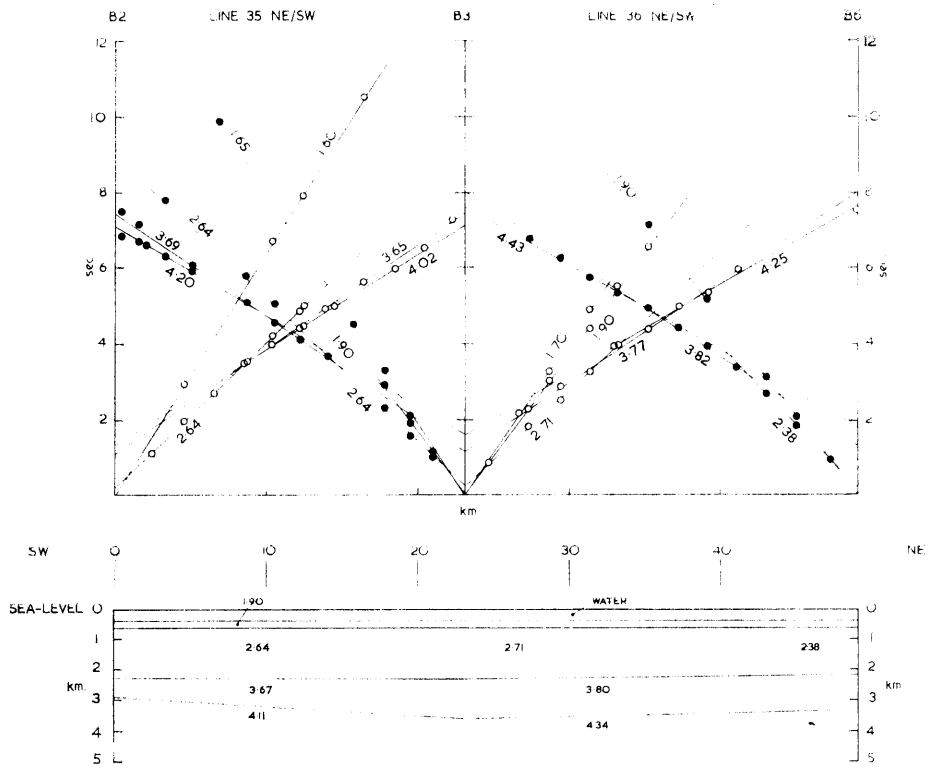

FIGURE 22

Time–distance graph and section; sonobuoy lines 35 NE/SW and 36 NE/SW.

As to the 8·53 km./sec. arrivals, the high velocity suggests that they are derived from the top of the mantle, since there is nothing in the configuration of the shallow layers to explain them. However, in view of the small number of points, no reliance can be placed on the value of 8·53 km./sec. as an indication of velocity or dip. Assuming a velocity of 8·2 km./sec., the depth has been calculated as 18·5 ±2 km. below sea-level.

b. *Sonobuoy lines 33 and 34; two-ship line 27.* Travel times for the sonobuoy lines, corrected for water delay are shown in Fig. 24. Line 33 is relatively straightforward, though a set of arrivals from the layer of velocity 4·02 km./sec. has to be assumed, shooting north-east, to match the reciprocal times of the 3·85 km./sec. alignment in the reverse direction. Line 34 shows faulting by displacement of the first arrivals in both directions of shooting and a satisfactory interpretation can be made on the assumption that this fault also affects the 4·93 km./sec. layer. Such layering can be carried farther south-west to the end of line 27 (Fig. 25), where alignments of apparent velocity 4·48 and 5·69 km./sec. are taken to be the up-dip velocities of the appropriate layers on lines 33 and 34.

When the shallow section had been established from the sonobuoy lines, a new datum was drawn within the 5·0–5·25 km./sec. layer, sloping from a depth of 5·24 km. at the south-west end to 2·74 km. at the north-east end of the line, and the times of the deeper refractors were corrected to this datum level (Fig. 25). The new travel times differ considerably from the old ones, in particular that they now show two separate alignments of about 6·0 and 6·6 km./sec. in each direction, clearly representing the layers of velocities 5·92 and 6·70 km./sec. already found on line 26. At the intersection of the two lines, depths agree to approximately 10 per cent.

At the north-east end of line 27, faulting is indicated by a displacement of the first arrivals on line 27NE together with a sudden decrease in trace amplitude. An increase in thickness of the sediments is not sufficient to explain the observed time step and displacement of the deeper interface is also necessary. First arrivals over the site of the faulting, shooting south-west, can be interpreted as showing two separate displacements, and it is likely to be a zone of faulting several kilometres wide along the line of section.

As in line 26, first arrivals beyond a range of 100 km., shooting south-west, fall on a line of high apparent

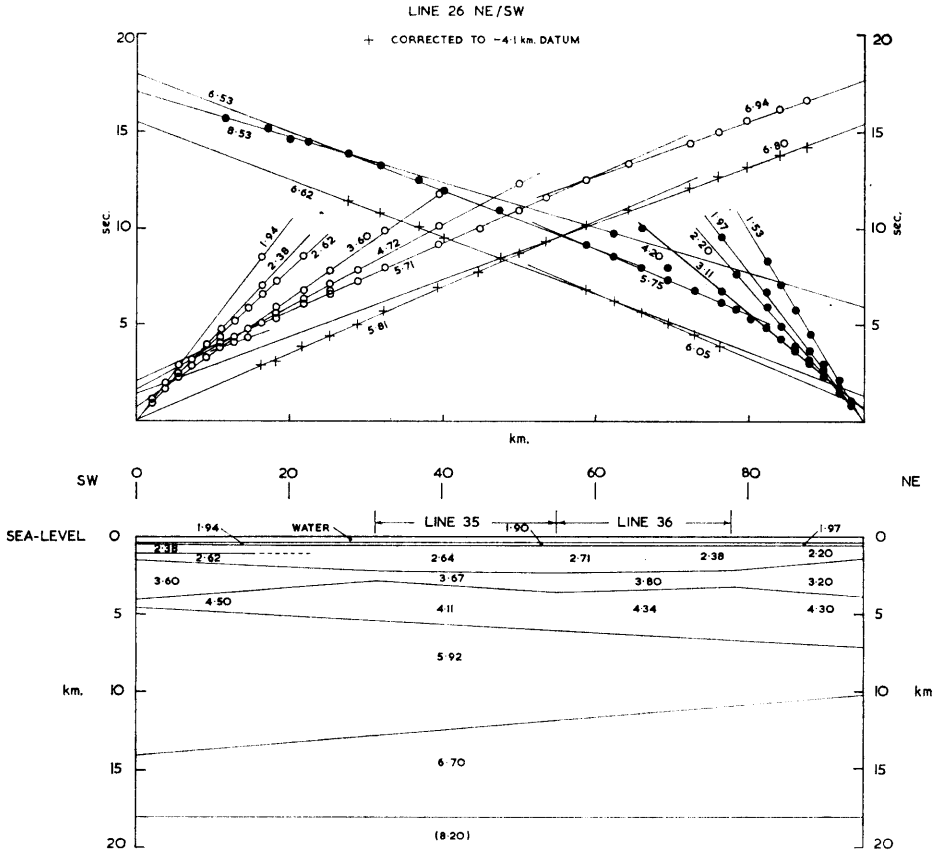

FIGURE 23

Time–distance graph and section; line 26 NE/SW. Crosses indicate first arrivals corrected to a datum at a depth of −4·1 km.

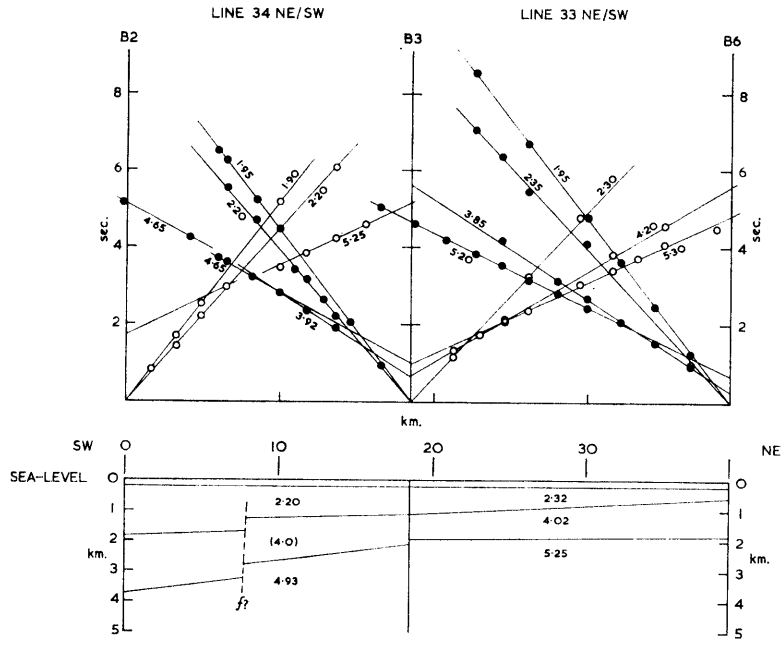

FIGURE 24

Time–distance graph and section; sonobuoy lines 33 NE/SW and 34 NE/SW.

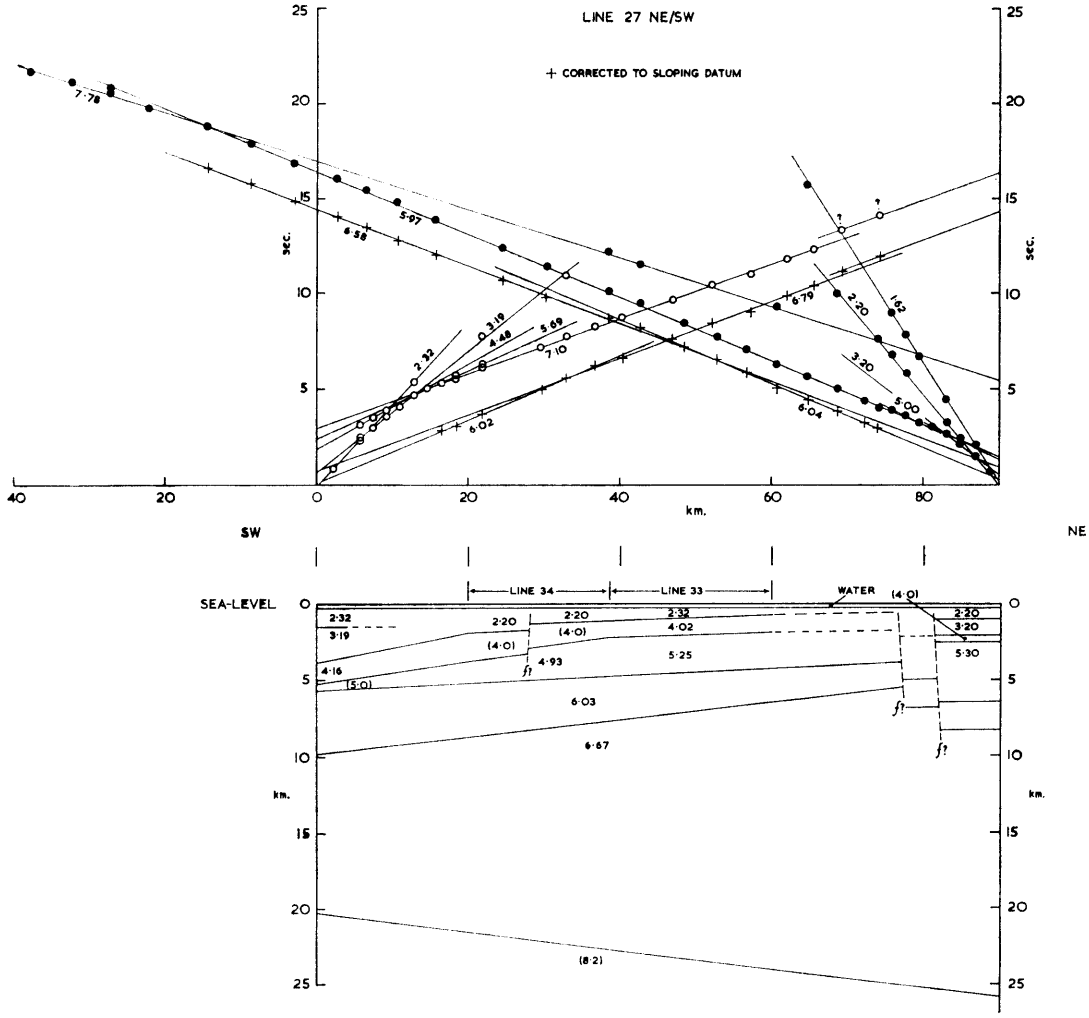

FIGURE 25

Time–distance graph and section; line 27 NE/SW. Crosses indicate first arrivals corrected to a sloping datum above the 6·03 km./sec. layer.

velocity (7·78 km./sec.) and these are assumed to be mantle arrivals. This apparent velocity can be explained by assuming that the sediments continue to thicken towards the south-west (i.e. over the top of the continental slope) at the same rate as over the south-western half of line 27. On the further assumption of a normal mantle velocity (8·2 km./sec.), it can be shown that the mantle must be rising to the south-west as depicted in Fig. 25. This configuration brings the mantle to within 1·5 km. of its depth on line 26 at the same position.

c. *Land–sea line 19.* This early land–sea line was shot from Nelson Island towards the north-west. The travel-time graph is shown in Fig. 26 but little can be deduced from this alone. If it is assumed that the arrivals come from the 6·03 km./sec. layer seen on line 27 and the delay through the section at the south-west end of that line is used, then the overall refractor velocity can be calculated. Assuming no delay at the receiver, a minimum velocity of 6·08 km./sec. is obtained, and this is comparable to the values obtained on lines 26 and 27.

An interesting point emerges when the sea-bottom profile for line 19 is plotted together with the section for the south-west end of line 27 (Fig. 26). A prominent terrace feature at the top of the slope to the trench then correlates exactly with the 2·32/3·19 km./sec. interface, suggesting that the 2·32 km./sec. layer (semi-consolidated sediment) has been built out across the shelf on top of the 3·19 km./sec. layer.

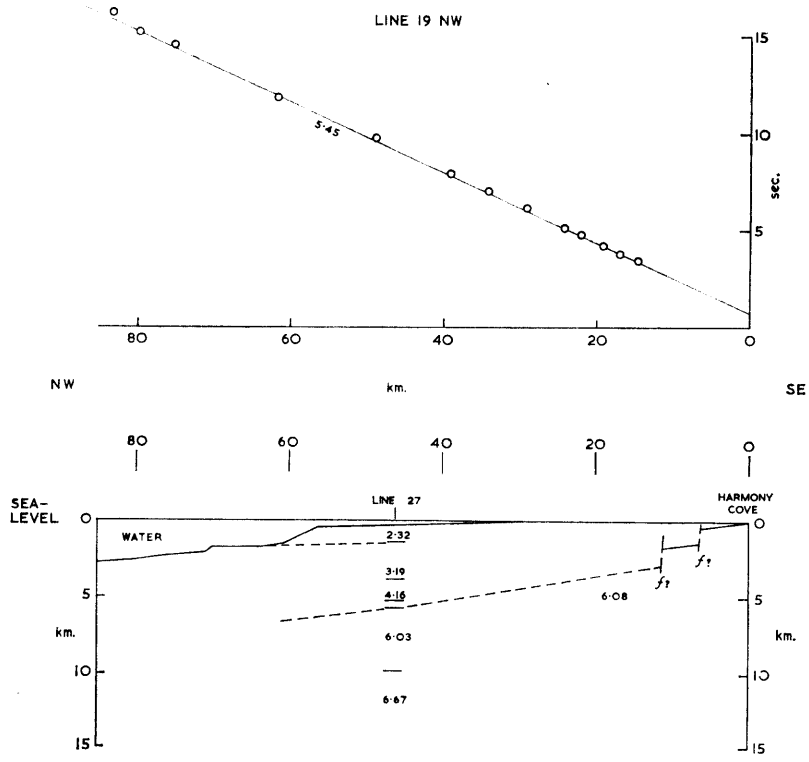

FIGURE 26

Time–distance graph and section; line 19 NW. A section from the south-west end of line 27 NE/SW has been inserted to indicate the general structure.

4. *The vicinity of Gibbs Island*

From the lines described so far and from the geology, it is clear that normal faulting parallel to the islands is a major structural feature of the south-east side of the South Shetland Islands from Livingston Island to the north-east as far as King George Island. A major point of interest, therefore, was to discover whether this continued to the north-east past Elephant and Clarence Islands. At the same time, Gibbs Island was suspected of being of structural interest because of its geology (p. 3-4), its association with a prominent east–west magnetic anomaly and considerable local sea-bottom topography.

Accordingly, a pair of two-ship lines (28 and 29) were shot approximately north–south as close to Gibbs Island as possible and with an overlap of 50 km. across the north-west edge of the "Bransfield Trough". The interpretation of these lines is not straightforward and several points require clarification. In the following account and in Fig. 27 the notation "28(N)", etc. is used as a convenient abbreviation for "the receiving point at the north end of line 28".

Travel times corrected for water delay only are shown in Fig. 27. Reciprocal times tie to about 0·1 sec. despite considerable drift of the receiving ship on the second day. The outstanding features of the plot are the upfaulted block extending from 10 to 25 km. south of 28(N) and the absence of any major faulting on the side of the trough. Instead, first arrivals on line 29N clearly indicate that variations in travel times over the deep water are controlled by sea-bed topography. For this reason, apparent velocities for the deep layers on this plot cannot be used to obtain true refractor velocities without first making considerable topographic corrections.

A similar approach was made in the interpretation of these lines as was made on lines 26 and 27. At each receiver station a section for the shallow layers was constructed down to the top of the 5·8 km./sec. layer, using the apparent velocities and intercepts taken from the graph in Fig. 27. When the shallow section at each station is plotted out relative to a local sea-bottom datum, the surprising fact emerges that the base of the 3·75–4·75 km./sec. layer is approximately flat over most of the line. This suggests that topographic variation across the north-west side of the "Bransfield Trough" between 28(S) and 29(N) is due to variations in the thickness of this layer.

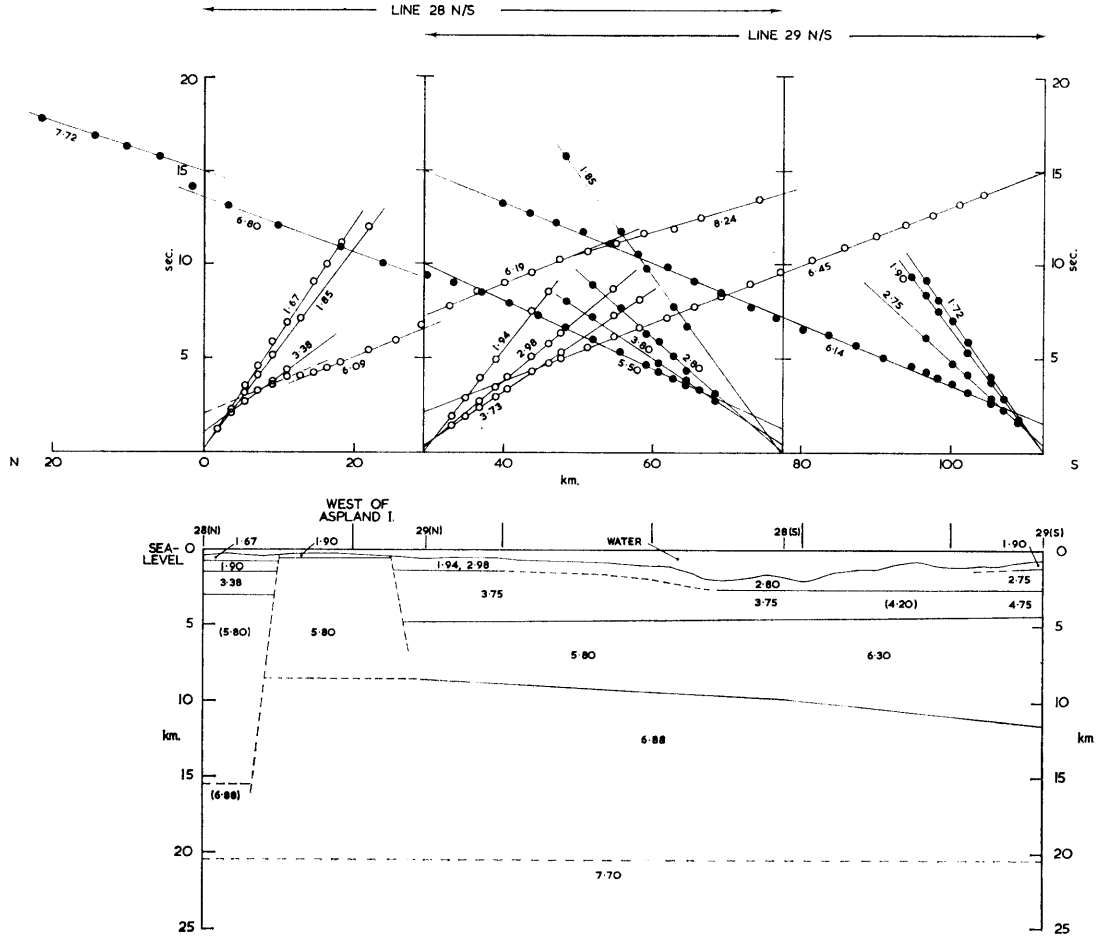

FIGURE 27

Time–distance graph and section; lines 28 N/S and 29 N/S. Times are corrected for delay in the water layer only.

Another feature of note is that the line of first arrivals on line 29N shows time deviations which correspond exactly with the sea-bottom topography, every rise or depression of the sea bed being marked by a corresponding delay or advancement in the travel times. The first arrivals, when corrected only for water delay, have a root mean square deviation of 0·13 sec. but, when they are corrected to a new datum on the assumption that the topography across the floor of the "Bransfield Trough" is due to the layer of velocity 2·8 km./sec., this is reduced to 0·05 sec. (Fig. 28).

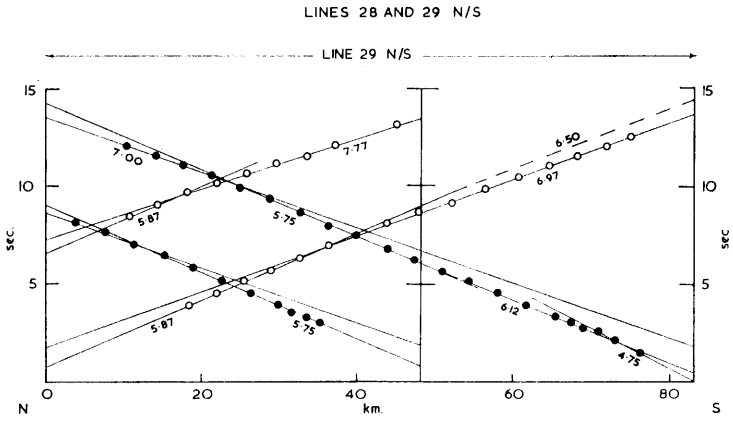

FIGURE 28

Time–distance graph for lines 28 N/S and 29 N/S corrected to a datum level at −2·7 km.

A new datum was drawn at −2·7 km., the level of the top of the 3·75 km./sec. layer at 28(S), and all first arrivals from the high-velocity refractors (>5·0 km./sec.) between the ends of line 29 were corrected to it. The new time–distance plot in Fig. 28 shows some surprising features. In general, there are now two alignments, one at about 6·0 km./sec. and one at about 7·0 km./sec. The 4·75 km./sec. arrivals at 29(S) are interpreted as evidence of a lateral change in velocity in the 3·75 km./sec. layer seen to the north; this, in turn, implies a velocity in the layer beneath certainly greater than the apparent velocity of 6·12 km./sec. and, in fact, approximately 6·30 km./sec. Such a lateral change in velocity at this level in the crust (from 5·80 km./sec. in the north to 6·30 km./sec. in the south) is supported by the change in apparent velocity seen on line 29N (6·12 to 5·75 km./sec.). In the reverse direction, line 29S, a corresponding change in the apparent velocity to 6·5 km./sec. is necessary to achieve a satisfactory reciprocal tie as indicated by the broken line in Fig. 28.

A second deeper refractor is indicated in Fig. 28 by lines of apparent velocity at about 7·0 km./sec. Making due allowance for the lateral velocity changes mentioned above, its velocity proves to be 6·88 km./sec. and its depth is about 10 km.

Turning to the faulted block at the north end, the observed time throw on the 6·09 km./sec. arrivals on line 28S is 0·7 sec. (Fig. 27) but, in order to translate this into terms of depth, information is needed about the shallow layers. Here it has been assumed that only Recent sediments of low velocity cover the 5·8 km./sec. layer, because the block is an extension of the ridge carrying the sheer rocky islands of the Gibbs Island group, implying well-consolidated rock at no great depth. If a velocity of 1·90 km./sec. is assumed for the sediment, it transpires that only 0·4 km. is required and this has been adopted in Fig. 27. Some support for this assumption comes from the fact that, on line 28S, the 1·67 and 1·85 km./sec. arrivals continue across the upfaulted part of the time–distance graph while the 3·38 km./sec. line does not, and in fact there is a real dearth of second arrivals in this part of the plot (Fig. 27).

The depths of the 5·80 and 6·88 km./sec. layers under the fault block and farther north have been calculated on the basis that such layering continues across this major fault zone. The apparent velocity of 6·80 km./sec. shown on line 28N across the fault block (Fig. 27) indicates that the deepest layer continues so far, but whether it exists beneath the shelf around Elephant Island at the north end of the section cannot be definitely stated on the present evidence.

With the aid of the bathymetric data, there is little difficulty in outlining the entire fault block. From Fig. 29 it can be seen that the Gibbs Island group stands on a prominent east–west ridge, and the linear east–west depression which divides it on the north side from the shelf around Elephant Island coincides

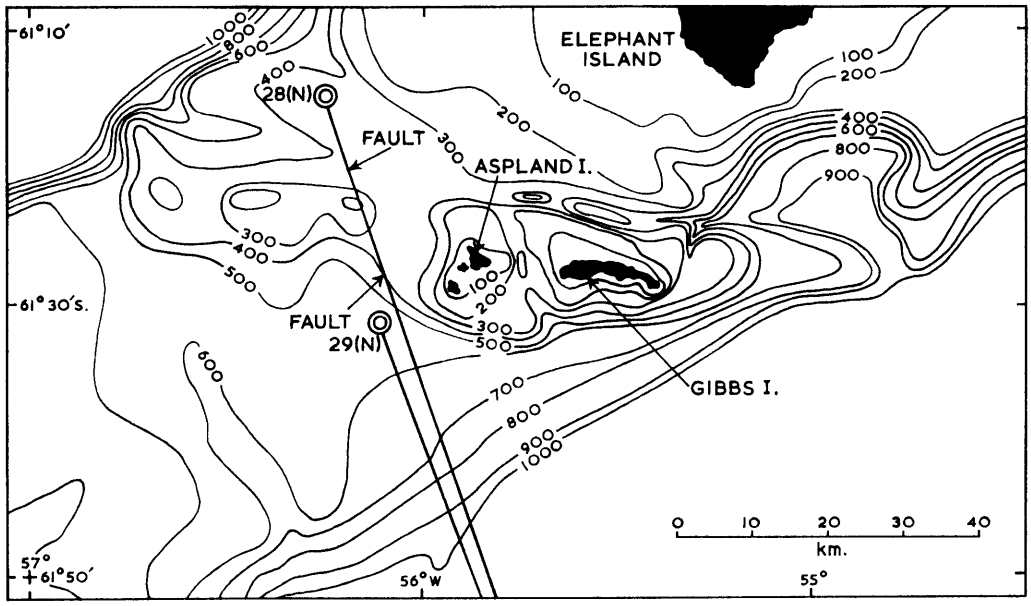

FIGURE 29

Bathymetric map of the Gibbs Island ridge. The locations of faults detected on lines 28 N/S and 29 N/S are also shown. The contours are at 100 m. intervals.

with the position of the northern fault in the section (Fig. 27). The position of the southern fault in the section corresponds to the slope defining the south side of the topographic block and it trends across the shelf from the continental slope in the west to the edge of the "Bransfield Trough" in the east.

Finally, mention should be made of the 7·7 km./sec. alignment at the end of line 28N (Fig. 27). If these points are assumed to be arrivals from the mantle, the total thickness of rock with a velocity of 6·8 km./sec. (thickness under shots and receiver combined) can be calculated as 17·8 or 15·5 km., depending on whether a velocity of 8·1 or 7·7 km./sec. is assumed for the mantle rocks. In the section of Fig. 27, 7·7 km./sec. has been assumed and the layer has been drawn flat at the uniform depth of 20 km. However, if its depth at the south end of the section is taken as about 15 km. (similar to the depth farther south-west on lines 24 and 25), the depth at the north end of the section (beneath the shelf surrounding Elephant Island) could be as much as 25 km.

VII. DISCUSSION OF THE RESULTS

1. *Velocity grouping*

The interpretation of the seismic results in geological terms requires first a translation of seismic velocities into their geological equivalents. Unfortunately the variation in compressional-wave velocity in the rocks of the crust is continuous and only very broad inferences can be made about a rock from a knowledge of its *P*-wave velocity alone. There are no precise velocity divisions that can be applied everywhere, but it may be that in any limited area certain groups can be separated out that are geologically significant. A plot of the frequency of occurrence of seismic velocities grouped in intervals of 0·1 km./sec. was made for this area (Fig. 30). In view of the limited number of determinations, running means of groups of three velocity occurrences have been plotted. The velocities encountered fall into the groups shown in Table II, in which probable geological equivalents are also given.

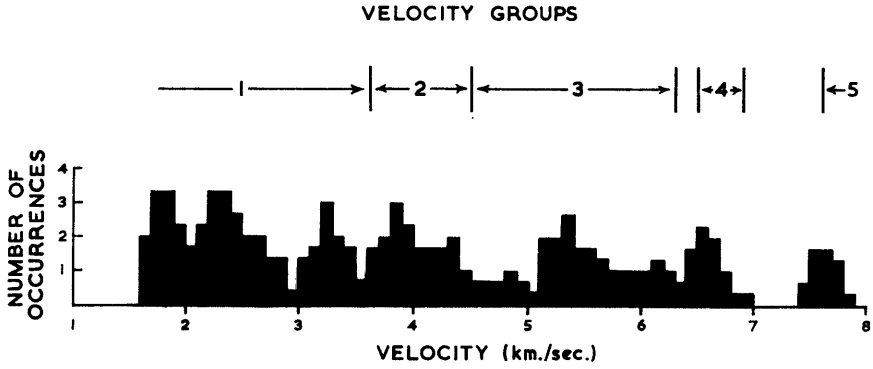

FIGURE 30

The frequency of occurrence of seismic velocities in the area of the survey. The number of occurrences was plotted at intervals of 0·1 km./sec. velocity and running means of three calculated for the plot shown here.

TABLE II

DIVISION OF SEISMIC VELOCITIES INTO GROUPS AND THEIR PROBABLE GEOLOGICAL EQUIVALENTS

Group number	*Velocity range* (km./sec.)	*Geological equivalent*
1	1·5–3·6	Unconsolidated and consolidated sediments
2	3·6–4·5	Volcanic rocks and/or consolidated sediments
3	4·5–6·3	Acid igneous and/or metamorphic rocks
4	6·5–6·9	Basic igneous and/or metamorphic rocks
5	7·6–8·2	Mantle rocks

To summarize the results and as an aid in discussion, Figs. 31–34 show four geological cross-sections, drawn along the lines shown in Fig. 1. In these sections, solid lines indicate boundaries established from the seismic work, while the broken lines linking various parts of a section represent speculative connections.

Section 1 has been compiled from the results of lines 22, 24, 25, 31 and 29. The structure of Bridgeman Island is quite speculative by analogy with Deception Island. Section 2 depends on the results of lines 20, 32 and 27, but under the deep ocean to the north-west a standard oceanic section has been assumed (Raitt, 1963). Section 3 has been assembled from the results of lines 26, 27 and 28, whereas section 4 depends on results from lines 16, 21 and 26. The rocks are grouped together on these sections according to the classification given in Table II.

2. *Distribution of sediments*

The present work enables a general estimate to be made of the thickness of sediment in two areas—Bransfield Strait and the shelf north-west of the South Shetland Islands.

From section 1 it is clear that at least 1·2 km. of undoubted sediment (1·84–3·3 km./sec.) is present in the "Bransfield Trough" between Deception and Bridgeman Islands. In view of the evidence for submarine vulcanicity in the bathymetry of the area (p. 4), a considerable amount of lava and tuff must also be present in these sediments, and the layer beneath (4·0 km./sec.) is perhaps a similar mixture of sediment and lava which is older and better consolidated. The total thickness of sediment may thus be as much as 2·5 km.

The variation in thickness of sediment across Bransfield Strait is known only along seismic line 20. Section 2 summarizes the interpretation, showing how the sediment thickens to a maximum of 3·5 km. under the top of the slope defining the south-east margin of the trough. The bathymetry of this area leads one to expect such thick sediments along much of the southern margin of the "Bransfield Trough" for a similar slope can be followed 70 km. to the south-east of line 20 and probably about 200 km. to the north-west.

The layers of velocity 1·8–3·3 km./sec. undoubtedly represent geologically young sediments which are in part unconsolidated. The source material is not hard to find in the Tertiary to Recent vulcanicity of the South Shetland Islands which must have poured out vast amounts of tuff in addition to material derived by the normal processes of marine erosion. The configuration of the wedge of sediment along the south-eastern margin of the "Bransfield Trough" suggests that it may have been derived by erosion of Trinity Peninsula at a time of reduced relative sea-level, with the formation of a complementary rock platform near the coast.

The layer of velocity 4·0 km./sec. shown in section 2 north-west of Trinity Peninsula is not precisely delineated, but there is no doubt that a considerable thickness of material of about this velocity overlies the igneous or metamorphic basement. At present its nature is obscure and geological investigation of the offshore islands and further geophysical work would be required to elucidate it. However, following the discovery of Cretaceous metasediments on the offshore islands at Cape Legoupil (Halpern, 1964), it is possible to speculate that the layer of velocity 4·0 km./sec. represents these same rocks. Such sediments could thus extend about 50 km. into Bransfield Strait and underlie the flat shelf area that extends offshore from Trinity Peninsula in this vicinity, and reach a depth of about 3–5 km. Alternatively, these shelves may have been built up by Tertiary vulcanicity and the resulting vents have been planed by marine erosion. Later discussion on the evolution of the crustal structure will attempt to bring out the importance of these shelves in reaching an understanding of this area.

The second area in which a certain amount of information on sediments has been gained is the shelf north-west of the South Shetland Islands. On section 2 only about 2 km. of sediment is shown 30 km. offshore from the islands, but farther south (section 4) the sediment thickens to about 6 km. if all layers of velocity less than 4·5 km./sec. are included. This approaches the maximum amount typically found on continental shelves (Worzel, 1968). Farther north-east along this shelf, off Elephant Island, 2·5 km. of sediment was found at the north end of line 28, so it seems likely that the entire shelf north-west of the islands has a cover of sediment 2–5 km. thick, except for the rock platform immediately adjacent to the islands themselves.

Certain other features emerge from the present work. Although velocity layering has been assumed in the sediments for the purposes of interpretation, since it enabled simple mathematical procedures to be

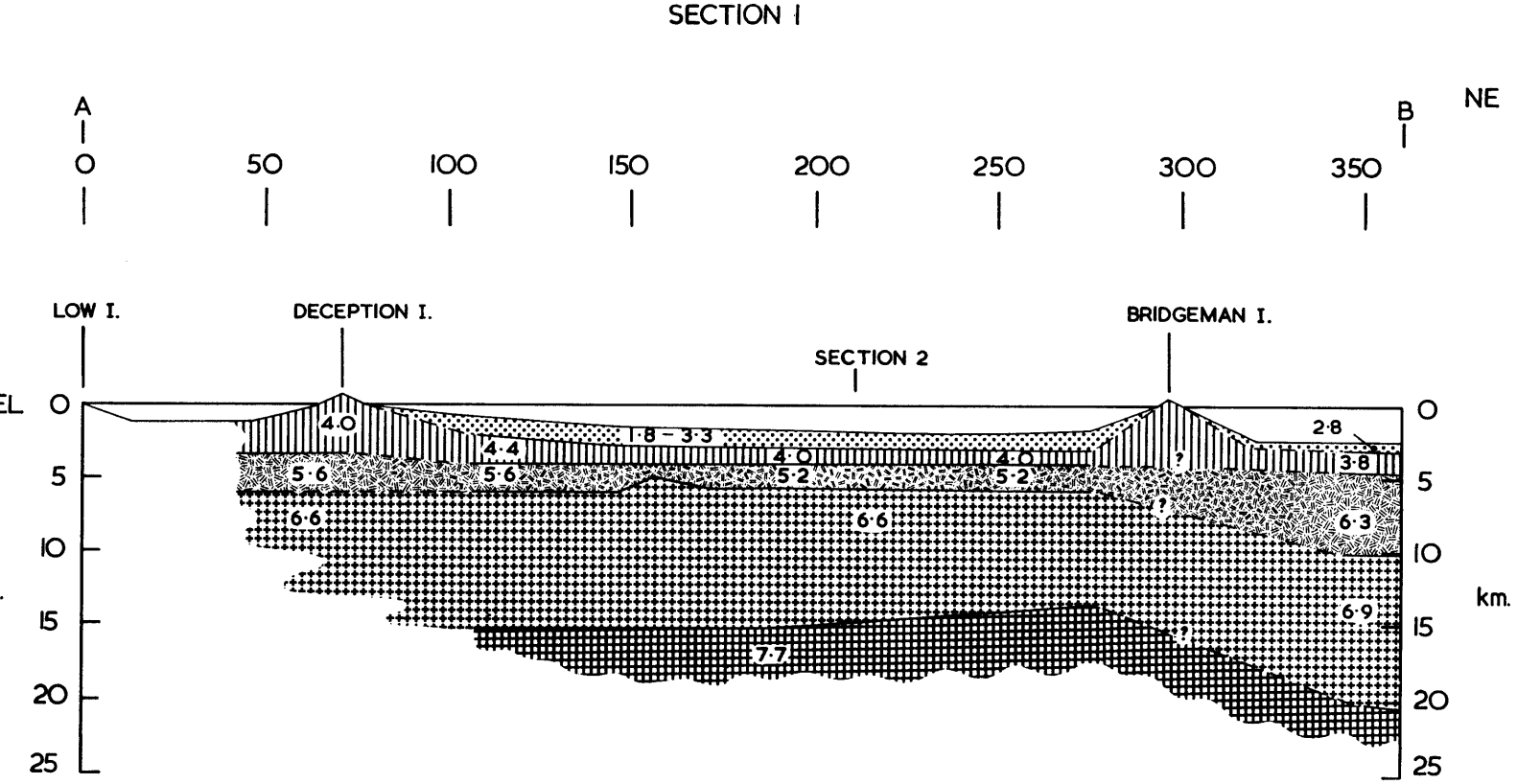

FIGURE 31

Generalized cross-section along line A–B (Fig. 1). Both in this figure and in Figs. 32–34 the solid lines represent interfaces for which there is some evidence from the present survey; the broken lines represent hypothetical connections.

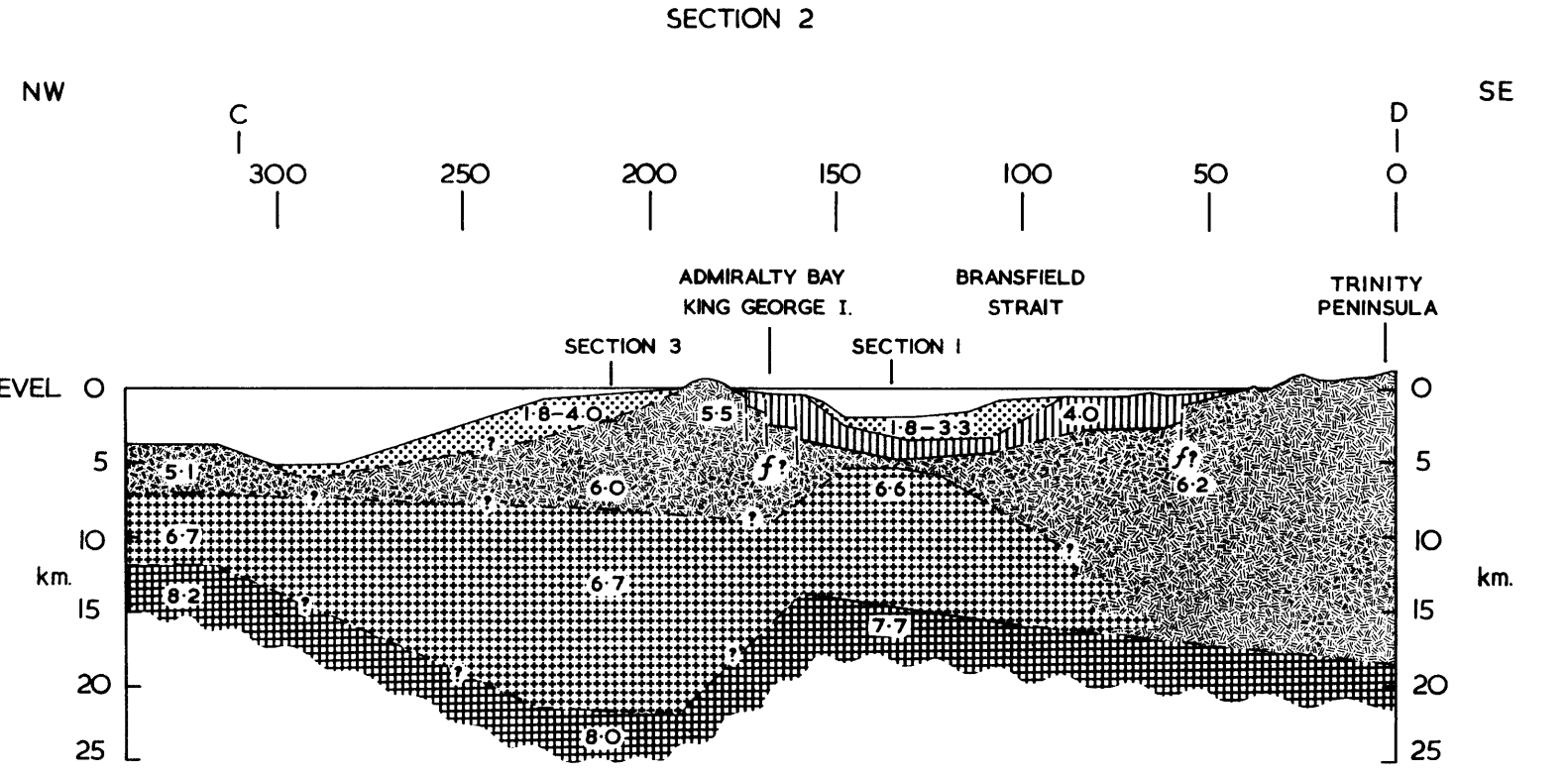

FIGURE 32

Generalized cross-section along line C–D (Fig. 1).

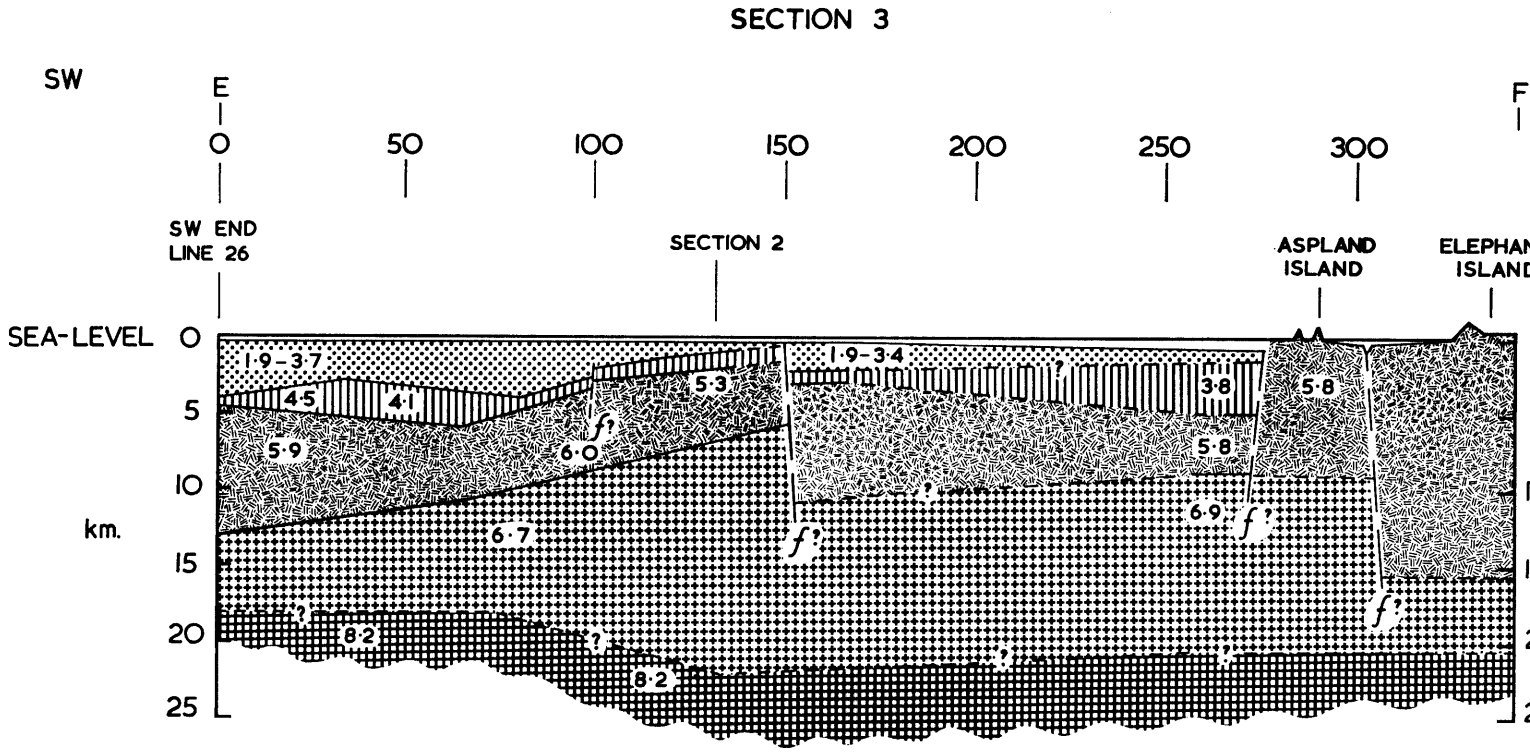

FIGURE 33
Generalized cross-section along line E–F (Fig. 1).

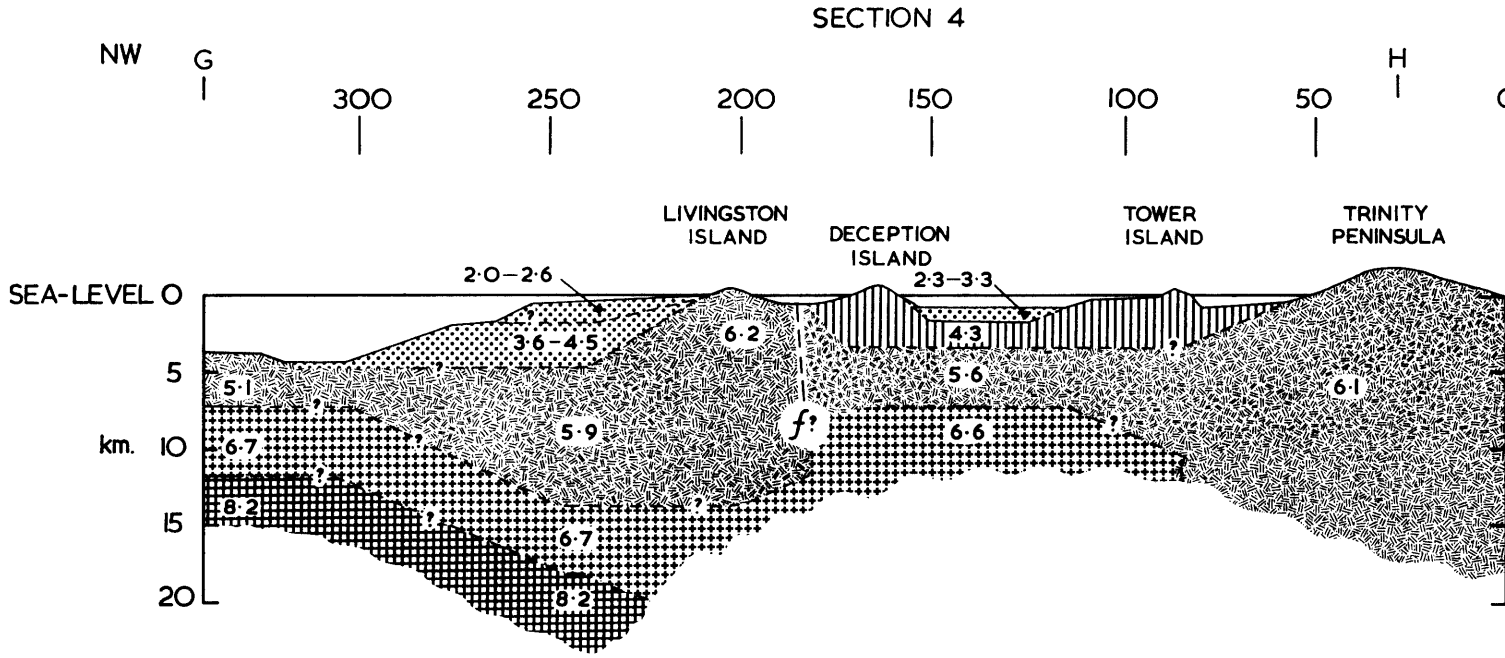

FIGURE 34
Generalized cross-section along line G–H (Fig. 1).

used, an attempt was also made to see whether any velocity–depth relationship could be discovered. The graph in Fig. 35 was prepared by plotting the depth below the sea bed to a layer of any particular velocity against that velocity. The result is comparable with a curve prepared by Nafe and Drake (1963) from the much more numerous results obtained off the east coast of the United States and it can be seen that there is broad agreement with the present data.

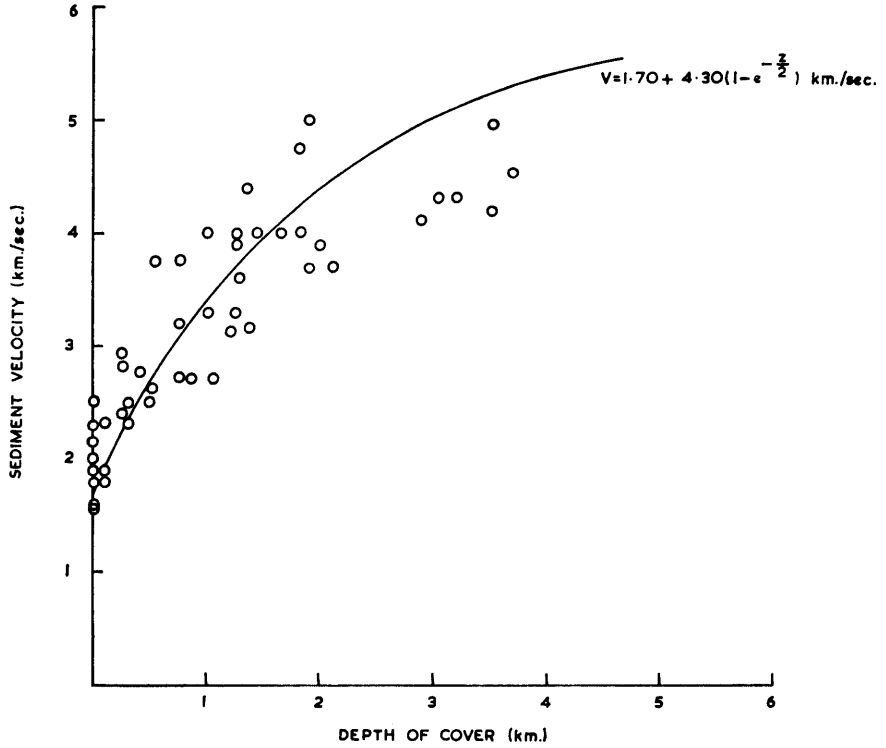

FIGURE 35

A plot of seismic velocity versus depth (to the top of the layer) for sedimentary layers within the area of the survey. These data may be compared with a curve derived by Nafe and Drake (1963) for the east coast of North America.

There are other points of comparison with the continental shelf off the eastern United States. In both areas the sediment thickens steadily towards the edge of the shelf and much of it is either unconsolidated or semi-consolidated. For instance, in the middle of line 26 there are about 2 km. of sediment of velocity 2·7 km./sec. or less, thinning to only 0·5 km. at the landward end of line 27. Moreover, the bathymetric profile of line 19 suggests that some of the sediment layers crop out as terrace features on the continental slope in a similar way to those off the eastern United States (Drake and others, 1959).

More detailed comparison and consideration of the relation of the sediment to the trench must await further investigation, and this could prove to be an important area for study by the seismic profiling technique. At the present time it is apparent that this shelf has resulted from long continued sedimentation. Similar shelves, in places as much as 150 km. wide, border the Antarctic Peninsula for several hundred kilometres southwards as far as the Bellinghausen Sea, and they may well be the sites of major accumulation of sediments.

The source of the sediments in this area must be sought in the neighbouring islands. The history of the islands as an upstanding landmass probably began around Triassic times (Orlando, 1968). At the south-western end of these islands the (?) Carboniferous greywacke-facies sediments of Miers Bluff had already been folded and may have been subjected to some erosion. The main uplift of the South Shetland Islands must have taken place in early Tertiary times as a result of intrusion of the major Andean batholiths of Livingston and King George Islands. These could well have yielded a source for Mesozoic and Tertiary sediments, but it is difficult to visualize them as the source of the deeper layers of relatively high velocity (4·0–4·5 km./sec.). Some indication of the age of these sediments can be gained by using a general

relationship between seismic velocity, depth and age for undisturbed sediments (Faust, 1951). By applying this relationship to the sediments of line 26, the ages of the various layers were found (Table III).

TABLE III
AGES OF THE SEDIMENTS NORTH-WEST OF THE SOUTH SHETLAND ISLANDS

Layer velocity (km./sec.)	*Depth* (km.)	*Age*
1·8–2·0	Surface	Tertiary
2·6	0·5–1·0	Cretaceous-Tertiary
3·6	1·5–2·5	Upper Carboniferous–Cretaceous
4·3–4·5	3·0–4·0	Carboniferous

These values seem to be appropriate for the upper layers, and for the deeper rocks they raise the interesting possibility that there may be relatively undisturbed late Palaeozoic or early Mesozoic sediments at the base of the sedimentary column. This has perhaps remained not only unaffected by severe folding, but also by the Andean intrusions which are confined to a narrow zone along one side of the island block where there has always been active vulcanicity, causing uplift only along that zone to form the present island chain. The source of these sediments and of the Miers Bluff Series of Livingston Island will be discussed later (p. 38-41).

Finally, lines 28 and 29 throw some light on the distribution of sediments across the north-east end of the "Bransfield Trough" (Fig. 27). The shelf to the north-west of the trough is not upfaulted relative to the trough in the same way as the South Shetland Islands farther south-west. Instead, the steep slope forming that side of the trough seems to mark a thickening of the 3·73–3·98 km./sec. layer on the shelf. The absence of magnetic anomalies over this shelf suggests that this layer is sediment, presumably derived from erosion of the islands and spread across this area by currents as a flat sheet, which is now as much as 5 km. thick in places. In contrast, the trough is floored with rock of velocity 2·8 km./sec., probably poorly consolidated volcanic material of fairly recent origin, since it has a very rugged relief rising in one place in a large seamount nearly 2,000 m. high. The general configuration of the shallow layers in Fig. 27 suggests that a previous wider and deeper trough is being progressively filled from the sides by sedimentation and by sporadic volcanism along the centre.

3. *Acid igneous and/or metamorphic rocks*

All of the rocks in the velocity range 5·3–6·2 km./sec. are included here. Both field and laboratory investigations of compressional-wave velocity have shown that a great variety of rocks falls within this velocity range, including most acid and intermediate igneous and metamorphic rocks commonly exposed in the upper part of the continental crust as well as some lavas and low-grade metasediments (Birch, 1960). Their distribution in this area will now be briefly reviewed. Much evidence for major faulting affecting rocks at this level in the crust has been found in the present work but this will be discussed in more detail later (p. 36–38).

The distribution of these rocks is summarized in sections 2, 3 and 4 (Figs. 32–34) which show that they are best developed in two areas—along the line of Trinity Peninsula and along the line of the South Shetland Islands—but in between, beneath Bransfield Strait, they constitute a relatively small part of the crust.

Along the coast of Trinity Peninsula, rocks of this group appear to extend to a depth of 18 km. for both land–sea lines 18 and 20 showed first arrivals of apparent velocity 6·0 km./sec. extending about 50 km. into the strait. There can be no doubt that these refer to the metasediments and batholithic intrusions of the peninsula. A gradational junction is postulated against the rock of velocity 6·6 km./sec. found at a high level under the strait (section 2).

There is a complex situation beneath the South Shetland Islands and this is only revealed rather sketchily

by the present data. At the south-western end of the islands, rocks with the comparatively high velocity of 6·2 km./sec. occur close to the surface along the south-east coast of Livingston Island and under the rather deep water between this island and Deception Island. Deception Island itself seems to be a pile of lavas resting on crust of velocity 6·2 km./sec. and this possibly extends northwards under the shallow water towards Livingston and Snow Islands. However, to the east, south-east and south the 6·2 km./sec. crust does not extend far (no farther than the submarine slope surrounding Deception Island) and a 5·6/6·6 km./sec. layering is found. Bathymetrically, the area south of Deception Island may be regarded as a bridge across the "Bransfield Trough" at this point (Fig. 2). This bridge seems to be due mostly to a thickening of the 5·2–5·6 km./sec. layer and considerable thickening of the 4·0–4·3 km./sec. layer (cf. Figs. 32 and 34). The structure suggests that the bridge was built by volcanic activity, perhaps from several vents scattered across the area. A geological investigation of Austin Rocks might throw light on this point.

On the shelf north-west of Livingston Island, the acid rocks maintain a considerable thickness (10 km.) beneath the sedimentary cover.

King George Island, at the other end of the main group of islands, shows a lower crustal velocity (5·5 km./sec.) under the mantle of Tertiary volcanic rocks along the south-east coast. This may be due to Jurassic volcanic rocks which are known to crop out in the centre of the island.

Farther north-east, in the vicinity of the Elephant and Clarence Islands group, the results of lines 28 and 29 suggest that acid crust thickens to at least 15 km. and possibly as much as 20 km. beneath Elephant Island (section 3). Under the shelf between Elephant and King George Islands about 5 km. of acid crust occurs under sediments 3–5 km. thick. Strong evidence was obtained for the presence of major east–west faults isolating the Gibbs Island group, a topic that will be discussed in more detail later (p. 36–38).

One point that emerges from this distribution of rock types is the fact that, wherever there is a considerable thickness of acid crust, the surface geology shows geosynclinal sediments intruded by Andean igneous rocks. This is so on the Antarctic Peninsula and on Livingston Island; on Elephant Island the geosynclinal sediments, at least, are present though no Andean intrusions have been proved (p. 4).

If acid crustal rocks are thick along the line of the Antarctic Peninsula and the islands, it is clear from sections 2 and 4 that rocks of this velocity group are correspondingly thin under the deeper parts of Bransfield Strait. Beneath the peninsula the thickness of the Trinity Peninsula Series is at least 13·7 km. (Aitkenhead, 1965), and the total thickness after folding and intrusion or replacement by Andean batholiths must have been much more than this, though by now a considerable amount will have been lost by erosion. It seems reasonable to regard the total thickness indicated in section 2 (18 km.) as representing the approximate dimensions of the compressed geosyncline at the present time. Beneath the south-western end of the South Shetland Islands there would appear to be a maximum of 15 km. of similar rocks.

At the same time, the present seismic results from the "Bransfield Trough" indicate a maximum of only 2 km. of rocks of the appropriate velocity range (5·2–6·3 km./sec.) under the deep central part, though around Deception Island where the water is shallower they appear to thicken to 3 km. (section 4).

Thus there is no indication that rocks of the Trinity Peninsula Series occur under Bransfield Strait in comparable thicknesses to those on either side. This, of course, does not mean that sediments of the same age may not occur in the 5·2–5·5 km./sec. layer or the layer above, but it would appear that there was never a geosyncline in that location.

There emerges a two-fold linear distribution of acid crust in this area and this is one of the key features to be accounted for in any explanation of the crustal structure.

4. *Basic igneous and/or metamorphic rocks*

One of the striking features of this area is the widespread occurrence of rocks in the velocity range 6·5–6·9 km./sec. at quite high levels in the crust. Arrivals from this refractor form the main part of the time–distance graphs of all the longer lines in the area. Explosion seismic work since World War II has shown that rock of this velocity forms the main part of the crust under the ocean basins, where it probably represents a layer of basic igneous rock. Laboratory determinations of seismic velocity give a mean value of 6·8 km./sec. for basic igneous rocks, which are clearly distinguishable from acid igneous and metamorphic rocks (Birch, 1960). The lower part of the continental crust commonly shows similar velocities (Kosminskaya and Riznichenko, 1964), but there it may represent very high-grade metamorphic rocks of intermediate composition (Belousov, 1966; Ringwood and Green, 1966).

In the region discussed here, such rocks occur at particularly shallow depths in Bransfield Strait, being found beneath the area of deep water for a distance of nearly 250 km. at a depth of between 5 and 6 km. and with a velocity of about 6·6 km./sec. To the north-west, beneath the South Shetland Islands, there appears to be an abrupt and steep junction with the more acid crustal rocks. These rocks are next seen under the shelf to the north-west of the islands at a considerably greater depth, as much as 15 km. at the south-west end (section 4), and with a velocity of about 6·7 km./sec. To the south-east, beneath the Antarctic Peninsula, the nature of the contact with the thick acid crustal rocks is obscure.

The presence of this rock layer at shallow depth under Bransfield Strait invites comparison with the standard section of the oceanic crust (Raitt, 1963). In Bransfield Strait, the water is shallower, there is more sediment, the 6·6 km./sec. layer is thicker and the mantle has a lower velocity than in the standard oceanic section. Nevertheless, the structure is much more akin to that of the ocean basins than the continents, notably in the absence of more than a few kilometres of acid rocks and in the shallowness of the mantle.

Farther north-east, in the vicinity of Gibbs Island, section 1 (Fig. 31) shows how the basic layer is again prominent, though rather deeper at about 10 km. and with a rather higher velocity of about 6·9 km./sec. However, its thickness is uncertain, for mantle arrivals were unreversed here and the thickness shown in section 1 (Fig. 32) could well vary by as much as 5 km. (p. 29).

5. *Mantle rocks*

Explosion seismology in the last 20 years has shown that the mantle varies considerably in velocity from the mean value of 8·2 km./sec. found under stable areas of the continents and ocean basins. Beneath active areas, low mantle velocities (down to about 7·6 km./sec.) are commonly found (Cook, 1962; Pakiser and Steinhart, 1964). The best evidence for the presence of rock of this velocity range comes from Bransfield Strait where both the two-ship lines (24 and 25) and the land–sea lines (18 and 20) can be consistently interpreted with a layer of velocity 7·6–7·7 km./sec. at a depth of about 14 km. (sections 1 and 2).

The strength of the evidence has already been assessed (p. 14-15); the velocity of this layer is known only to $\pm 0 \cdot 15$ km./sec. and its depth to $\pm 1 \cdot 5$ km. The results of lines 24 and 25 in Bransfield Strait suggest that it maintains a depth of $14 \cdot 0 \pm 1 \cdot 5$ km. along most of the rest of the strait, so that it parallels the surface of the 6·6 km./sec. layer in forming an upstanding ridge. The depth beneath Trinity Peninsula fits the travel-time data of land–sea line 20NW, but it must be regarded as most uncertain ($\pm$ 2 km.) in view of how little is known of mantle and crustal velocities there.

North-west of the South Shetland Islands, mantle arrivals were again detected on lines 26 and 27, but with no satisfactory reversal. In section 2 this interface has been connected to the top of the 7·7 km./sec. layer in Bransfield Strait, but the little available evidence on mantle velocities north-west of the islands suggests that it is higher, around 8·0–8·2 km./sec. (line 26). This raises the whole question of where to draw the top of the mantle, a problem frequently encountered in active areas. If rock with a velocity of 8·2 km./sec. and density of 3·27 g./cm.^{3} (Worzel and Shurbet, 1955) were to occur under Bransfield Strait, it might be anywhere between 40 and 60 km. deep depending on the density assumed for the 7·6 km./sec. part. Current ideas on the processes involved suggest that there may be no interface but a transition into material of higher velocity (Cook, 1962; Ringwood and Green, 1966).

Possible mantle arrivals were again found under lines 28 and 29 south-west of Elephant and Clarence Islands, but here the evidence is least strong, consisting only of a single line of four first arrivals. Since there is no reversal, refractor velocity is not accurately known, but the depth here proves insensitive to refractor velocity and the depth shown is a minimum to rock within the range 7·6–8·2 km./sec. As explained on p. 29, it could be considerably deeper under Elephant Island and correspondingly shallower under the "Bransfield Trough".

6. *Faults*

A summary of the faults found in the present work or postulated on general grounds is given in Fig. 2.

Mainly from gravity data, Griffiths and others (1964) postulated the existence of a major fault bounding the south-east side of the South Shetland Islands and with a downthrow of about 4 km. to the south-east into Bransfield Strait, in the vicinity of Deception Island. This has been confirmed on lines 17 and 21 (arc) where the minimum throw of the fault is 2·5 km. on the main crustal layer (velocity 6·2 km./sec.). The

faulting indicates considerable uplift of the islands relative to Bransfield Strait, probably associated with the emplacement of the Andean granodiorite batholith of Livingston Island.

Farther north-east, along the steep topographic slope bounding the islands, there is evidence on lines 18 and 20 for considerable multiple faulting, all faults with downthrows to the south-east and with a total throw of 2–3 km., measured on the surface of the 5·5 km./sec. layer. Although these faults have been inserted as the result of a particular interpretation of one-way time–distance graphs, geological mapping has revealed extensive north-east to south-west faulting on the islands themselves (e.g. controlling the shape of Admiralty Bay) and the faults on the seismic section represent a logical offshore extension of this structural style. Similar remarks apply to the faults shown off the north-west coast of Trinity Peninsula.

Faulting undoubtedly affected the South Shetland Islands throughout Tertiary times. The latest faults cut the Point Hennequin Group of Tertiary lavas, but it is likely that the same tensional forces determined the sites of the volcanoes in the first place and of the Recent volcano on Penguin Island. A comparable line of vents probably existed off the north-west coast in Tertiary times and it seems likely that the sediments off that coast are downfaulted against the islands. The islands themselves must then have the form of an upfaulted block confined strictly to the zone of Andean plutonic intrusion.

Such evidence of long-continued normal faulting indicates a history of tension in this area through Tertiary times up to the present. The latest manifestation of this would seem to be the development of submarine volcanoes along a line of weakness between Deception and Bridgeman Islands (p. 4), and possible fault lines based on bathymetric evidence have accordingly been inserted in Fig. 2.

It might be expected that this major zone of faulting, so clearly defining the margin of the "Bransfield Trough" off King George Island, would continue north-eastwards, marking the edge of the deep water south of Gibbs Island. However, the results of seismic lines 28 and 29 (Fig. 27) show no indication of displacement of the main crustal layers at the edge of the trough as indicated above (p. 26).

Since the north side of the trough appears to be unfaulted here, it is probable that the faulting recorded off King George Island stops against a cross fault, and the presence of a volcano as large as Bridgeman Island suggests that such a cross fault may lie under it in the position shown in Fig. 2. Although section 1 (Fig. 31) also suggests a considerable change in crustal thickness across this line, it should be noted that the thickness north-east of Bridgeman Island is not well determined and could be several kilometres less.

On the south-east side of Bransfield Strait, a similar set of normal faults is associated with the block uplift of Trinity Peninsula. These appear on lines 20 and 18 with downthrows of 1 or 2 km. to the north-west (Figs. 10 and 11). The trend of these faults cannot be directly determined from the seismic results but, by analogy with the "O'Higgins fault" found by Halpern (1964) on the coast at Cape Legoupil, they have been shown trending parallel to the arc.

Farther north, in the Elephant and Clarence Islands group, large faults have been proved to flank the topographic ridge on which the Gibbs Island group stands (p. 28-29). The close correspondence between linear topographic features and the observed positions of the faults on the seismic lines deserves some emphasis, but there is other evidence which strongly supports the case for major dislocations here. First, there is the geology of Gibbs Island itself, which is formed mainly of chlorite-albite-sericite-schists striking approximately east–west, together with a schistose serpentinized dunite. The presence of serpentine bodies in an orogenic belt is generally an indication of large-scale faulting. Hess (1955) has emphasized their close relationship with deep shear zones in regions of Alpine folding, typically associated with low-grade metamorphosed sediments. The commonly held view is that large lensoid bodies of serpentine have been squeezed into their present positions from great depth along major shear zones (Lappin, 1966). Some indication of the trend at depth of such a shear zone beneath Gibbs Island can be gained from a magnetic survey in that vicinity (Ashcroft, 1967). A prominent east–west magnetic anomaly of about 1,000 γ amplitude associated with the island can be interpreted in terms of a thin planar magnetized zone dipping southward, and perhaps this is a set of dunite lenses lying in the shear zone.

On the basis of a strong relationship between faulting and topography in the vicinity of Gibbs Island, a case can be made for suggesting that the Elephant and Clarence Islands group as a whole is broken up by large transcurrent faults. The following summary of structural trends and bathymetry in this area should be considered.

Elephant Island: strike east–west, in the north.

Cornwallis Island: strike east–west; joined to Elephant Island by a flat shelf area.

Clarence Island: strike north-north-east; separated from Elephant Island by a rift about 1,800 m. deep.

Gibbs Island: strike east–west; separated from Elephant Island by a linear east–west depression marking a major fault.

Aspland and O'Brien Islands: strike north–south; separated from Gibbs Island by a linear depression 300 m. deep and from surrounding shelves by large east–west faults.

The diversity of strike direction in this area deserves some emphasis. It contrasts with the general continuity in trend observed along the other ridge of the arc in Trinity Peninsula and Joinville Island or with the rest of the South Shetland Islands to the south-west, and suggests that actual rotation of crustal blocks may have taken place as a result of transcurrent faulting.

Finally, mention should be made of the large fault zone shown near the north-east end of line 27 (Fig. 25). This has a total downthrow to the north-east of approximately 2·5 km. and it is possible that its trend is shown by the smoothed total-field magnetic anomaly over the South Shetland Islands (Griffiths and others, 1964). The anomaly rises steadily in magnetic field strength along the length of the islands towards the north-east, ending in a relatively sharp flank trending 290° off the north-west coast of King George Island; this corresponds almost exactly to the position of the fault at the north-east end of line 27. On this basis, a fault with the appropriate trend has been inserted off the north coast of King George Island (Fig. 2).

VIII. DISCUSSION ON THE CRUSTAL STRUCTURE

In any hypothesis explaining the evolution of the crustal structure of this region, the following points should be taken into consideration:

i. The bathymetric features mentioned on p. 4–5, and notably the sudden termination of the "Bransfield Trough" at its south-west end and the subdued trench north-west of the South Shetland Islands.
ii. The geological relations outlined on p. 3–4.
iii. The evidence, from the present seismic results, of large-scale transcurrent faulting in the area of Elephant and Clarence Islands which apparently caused rotation of crustal blocks.
iv. The concentration of thick acid crustal rocks in two linear zones beneath Trinity Peninsula and the South Shetland Islands, as shown by the present seismic results.
v. The thinness of acid crustal material under Bransfield Strait and the fact that the crustal structure there more nearly resembles that of a modified oceanic crust than continental crust.

There is little doubt that the main concentration of acid crustal rocks beneath Trinity Peninsula represents the Upper Palaeozoic geosynclinal belt in which the Trinity Peninsula Series was deposited, and which is now folded and intruded by Andean batholiths. However, the relation between these rocks and similar acid rocks which occur in considerable thickness (15 km.) beneath Livingston Island and the Elephant and Clarence Islands group is not yet clear. A direct link under Bransfield Strait cannot be sought, for here the crust, though intermediate in type between oceanic and continental, is closer to the oceanic type. Simple removal of an intervening strip of continental crust seems ruled out at once because, as Officer and others (1959) have pointed out in the case of the Venezuela Sea, this would imply uplift and erosion of about 25 km. of continental crust followed by submergence to a depth of 5–6 km. and deposition of 2·5 km. of sediment. There is nothing in the geology of this area to suggest such a tremendous revolution.

A possible alternative mechanism is some form of erosion of the crust from below combined with basification of the rest to produce high-velocity crustal material at a shallow depth. Such a process has been invoked by Russian workers in the Sea of Okhotsk (Kosminskaya and Riznichenko, 1964). Apart from the serious isostatic problem raised by introducing basic igneous material into the crust on such a large scale, this would certainly not explain unique features of the structure such as its linearity and the abrupt termination of the "Bransfield Trough" against the shelf to the south-west.

There are two further hypotheses which might be put forward to explain the observed structure. The first would postulate that the South Shetland Islands and the Antarctic Peninsula had always occupied their present relative positions. Sedimentation in two parallel geosynclinal troughs during (?) Carboniferous times took place along the line of Trinity Peninsula and the South Shetland Islands. Both troughs then

underwent almost identical geological histories with severe folding of early Mesozoic date followed by volcanism in Jurassic times. Emplacement of Andean intrusions during the late Cretaceous–early Tertiary was accompanied by normal faulting and uplift, which has persisted to the present day. The folded and slightly metamorphosed geosynclinal sediments of very similar appearance are now exposed along Trinity Peninsula and at Miers Bluff on Livingston Island. These could be more or less contemporaneous deposits of the two geosynclines, although it has been suggested that the Miers Bluff sediments may be of a younger age. Under this hypothesis it is possible to explain points (ii) and (iv) given above, but not the others. It is also difficult to explain the variations in thickness of acid crust observed along the length of the South Shetland Islands and to visualize the manner in which the two troughs were filled by sediment.

The second hypothesis, which seems more probable, would postulate that the Upper Palaeozoic sediments on both the South Shetland Islands and the Antarctic Peninsula had been deposited in a single geosynclinal trough and shared the same geological history as a unit for a large part of geological time, for instance, sharing a common folding in the Mesozoic and vulcanicity in the Jurassic. At some later time, as part of a regional process of continental drift, a slice of the Antarctic Peninsula broke away and moved north-westwards relative to the peninsula to form the South Shetland Islands.

Among the merits of this hypothesis are that it relates the present area to the problem of the Scotia arc as a whole. For some time it has been recognized that the anomalous features of the arc (for instance, the geosynclinal sediments of South Georgia and the isolated continental rocks of the South Orkney Islands) can only be explained in terms of a former link between South America and Antarctica now disrupted by a process of continental drift. Hawkes (1962) has given one possible version of such a process. The general question will not be considered here but only the application of the principle as a means of explaining the structure of the crust in this area.

The most recent views on continental drift link this process to sea-floor spreading from mid-ocean ridges with associated sinking of crustal material along the sites of the oceanic trenches (Le Pichon, 1968; Morgan, 1968). In this context the subdued trench north-west of the South Shetland Islands implies sea-floor spreading of that part of the Pacific Ocean towards the south-east, though the complete absence of deep earthquakes in this area indicates that the system is at present inactive. But the relative movement of the islands and the peninsula at some time in the past could be envisaged as a drifting away of the Antarctic Peninsula towards the south-east in response to sea-floor spreading from the north-west, so that the South Shetland Islands block was left behind and a rift opened up in Bransfield Strait.

Perhaps the most striking piece of evidence in this area for drifting of the type postulated is the structural line trending north from Brabant Island through Boyd Strait (p. 4). This might well be put forward as the site of a sinistral wrench fault along which the south-west side of the island block had moved during drifting. Smith Island, which is directly across Boyd Strait from Livingston Island, is composed of "basement" rocks (personal communication from Dr. R. J. Adie), indicating an important structural break with the block of islands to the north-east. Bathymetrically, the continental shelf and slope north-west of Boyd Strait show complexities along the continuation of this structural line, though soundings here are inaccurate and conflicting. Farther north-west the trench axis has a definite displacement as if from a sinistral wrench fault passing through Boyd Strait. Moreover, there is a corresponding kink in the total-field magnetic anomaly published by Griffiths and others (1964), indicating possible displacement in the same direction.

At the north-east end of the South Shetland Islands it is not so easy to see a clear line of possible movement from the bathymetric evidence alone. Much transverse faulting has taken place in the vicinity of Gibbs Island but its dominant trend appears to be east–west, which would not account for the hypothetical south-east movement of the Antarctic Peninsula. Indeed, it is not as yet possible to see how the Elephant and Clarence Islands group fits into any pre-drift reconstruction, though in general terms the transcurrent faulting and rotation of crustal blocks that appear to have taken place must be closely associated with the process of drifting (p. 37-38). For the immediate purpose of fitting the islands back against the peninsula a clearer possibility is the fault line postulated as trending through Bridgeman Island (Fig. 2).

The question of the timing of the movements is extremely important. The physiographic features defining the structural lines mentioned above are unlikely to be older than Tertiary in age, for otherwise the submarine relief would have been smoothed by sedimentation. Bathymetrically, the line through Boyd Strait is linked to the narrow Gerlache Strait (500 m. deep) which separates Anvers and Brabant Islands from the Antarctic Peninsula (Herdman, 1948). Since these two islands are formed largely of Andean

intrusive rocks, it is probable that the abrupt features in the physiography of the area are no older than Tertiary. Similar arguments could be applied to the shear faulting in the Elephant and Clarence Islands group which finds such clear expression in their physiography. There is, of course, abundant evidence for tension in the whole area throughout the Tertiary in the form of normal faulting on both sides of Bransfield Strait, associated with widespread vulcanicity in the South Shetland Islands and in the "Bransfield Trough".

At this stage it is worthwhile examining this area more closely for some of the features that might be expected to be present if Bransfield Strait were a rift structure. For instance, some correlation might be expected between geological formations on opposite sides of the strait. However, it will be evident from p. 3–4 that since there are no formations striking across the arc such correlation is impossible. Some sort of geometrical match between opposite sides of the "Bransfield Trough" might also be expected for this is seen as the site of the actual split in the acid crust and intrusion of basic crust. Since this structure is so short, it is perhaps expecting too much to see an exact fit, but at first sight the difference between the straight south-east margin of the South Shetland Islands and the convolute edge of the shelf offshore from Trinity Peninsula could not be more extreme. However, it should be noted that the sea bottom offshore from Trinity Peninsula may have been severely modified since the original break took place. For instance, it is known from the present seismic data that the steep slope lying between depths of approximately 1,000 and 1,600 m. in the vicinity of lat. 62°36′S., long. 58°W. is built of low-velocity sediments and could be disregarded in attempting a fit. The flat shelves to the south-east could conceivably be the result of Tertiary vulcanicity, the vents subsequently being planed by marine erosion. Magnetometer profiles across these shelves show appropriate anomalies. Thus there may well have been a straight faulted margin on the south-east side of the trough which is now obscured by the later material of the shelves.

The hypothesis of rifting is made even more credible by comparing some of the features of the area discussed here with those of the Red Sea rift structure. Drake and Girdler (1964) have described the Red Sea as a main depression 200–300 km. wide and about 600 m. deep, floored by acid crust and downfaulted between large normal faults approximately corresponding to the present shorelines. Within this depression the acid crust is fractured by further normal faults parallel to the coasts. In the southern half of the Red Sea an axial fracture zone has developed, and this is marked by a trough averaging 55 km. in width, reaching depths of 2 km. and showing rough sea-bed topography. It is associated with magnetic anomalies of 2,000 γ amplitude and rock of unusually high seismic velocity (7·1 km./sec.) within 2·5 km. of the sea bed. This has been interpreted as a zone of incipient separation of the acid crust, accompanied by intrusion of basic igneous rocks, which is the first stage in the formation of new ocean crust.

It is possible to imagine the Bransfield Strait area as an asymmetric version of the same type of structure. The "Bransfield Trough" could be regarded as the central fracture zone, its width being 40–50 km. and its depth about 2 km. The topography in the "Bransfield Trough" is in general not so rugged as in the axial zone of the Red Sea, but there is considerable relief especially in the area north-west of Bridgeman Island. Moreover, the trough is underlain by rock of velocity 6·6 km./sec. at a depth of only 3 km. below the sea bed and large linear magnetic anomalies, which are at present the subject of detailed study at Birmingham, occur along its axis. To the south-east is the complex shelf area, which is floored by acid crustal rocks that are repeatedly downfaulted off the coast of Trinity Peninsula in a way reminiscent of the faulted Red Sea margin. Some of the bigger marginal faults have been recorded in the land–sea seismic work (Figs. 10 and 11) but refraction shooting is not detailed enough to distinguish others which may exist between 40 and 60 km. offshore. As mentioned above, it is possible to regard this area as being largely built over at the present time by the (?) volcanic rocks and sediments of the shallow shelves. Previously it may have had a general water depth of about 700 m. as is preserved in the embayments of deep water cutting through the shelves, for instance to the south and east of Tower Island (Fig. 2). The width of this zone of faulted acid crust is about 70 km., i.e. comparable to the corresponding dimension of the Red Sea (100 km.).

To the north-west of the "Bransfield Trough" the marginal block-faulted zone along the edge of the South Shetland Islands is much narrower (only 10–15 km. wide), so that the whole structure is not symmetrical about the axial zone as in the case of the Red Sea. A diagrammatic section illustrating the type of structure envisaged for the "Bransfield Trough" and based on Figs. 32 and 34 is shown in Fig. 36.

On the basis of this hypothesis, it is possible to establish a tentative date for the rifting movement. The 5·5 km./sec. layer in the "Bransfield Trough" may be regarded as oceanic layer 2 material, probably basalt lava flows developed on top of the new oceanic crust, and on top of this layer is about 2 km. of sediment. Assuming a fairly fast rate of accumulation of 10 cm./1,000 yr., the bottom of the sediments and

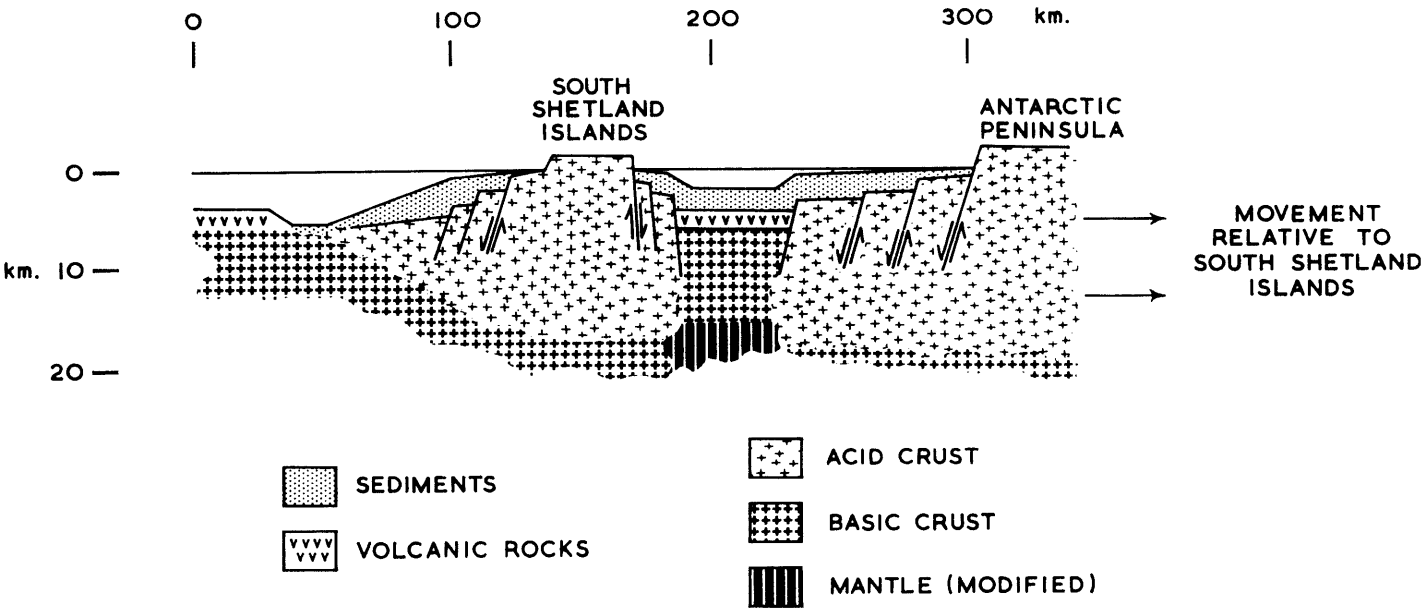

FIGURE 36

Schematic diagram illustrating the hypothetical origin of Bransfield Strait by a process of rifting.

hence the end of the main period of separation of acid crust would be about 20 m. yr. old. Further elucidation of time relations, especially with regard to any faulting in the sediments, could be gained by continuous seismic reflection profiling across the bottom of the trough. A great deal of faulting in the sediment, together with evidence for burial of considerable topography, would do much to reinforce the rifting hypothesis.

Although there is much that is still conjectural, this hypothesis might well account for the present structure over the main part of Bransfield Strait from Low Island in the south-west as far as Bridgeman Island 300 km. to the north-east. However, it is not clear at present whether this structure continues farther north-east past Elephant and Clarence Islands. The bathymetry of this area indicates that it does but the results from seismic lines 28 and 29 (p. 26) seem to indicate quite clearly that the steep north-west slope of the trough is not due to faulting. In this locality it seems that the trough is in the process of being filled by volcanic material (p. 34). In common with the shelf area offshore from Trinity Peninsula, this is one of the key areas for further investigation. For instance, it is possible that the interpretation of refraction lines 28 and 29 could be modified in the light of new information about the depth of sediments obtained by continuous seismic profiling over the north-west slope of the trough.

IX. ACKNOWLEDGEMENTS

THE author wishes to thank Sir Vivian Fuchs and the British Antarctic Survey for the facilities provided during the field operations. The helpful co-operation of Capt. D. H. Turnbull (R.R.S. *Shackleton*) and Capt. M. S. Ollivant, M.B.E., D.S.C., R.N. (H.M.S. *Protector*) and their ships' companies is gratefully acknowledged together with the assistance in the field provided by the other members of the University of Birmingham party, P. F. Barker, H. A. D. Cameron, P. Kennett and L. E. Parkinson.

The author is grateful to Prof. F. W. Shotton for laboratory facilities and to Prof. D. H. Griffiths, not only for assistance in the field but also for much helpful discussion of the work. Dr. R. J. Adie has assisted considerably in the preparation of the report.

Throughout the duration of the work the author was supported by a Natural Environment Research Council research studentship.

X. REFERENCES

ADIE, R. J. 1955. The petrology of Graham Land: II. The Andean Granite–Gabbro Intrusive Suite. *Falkland Islands Dependencies Survey Scientific Reports*, No. 12, 39 pp.

————. 1957. The petrology of Graham Land: III. Metamorphic rocks of the Trinity Peninsula Series. *Falkland Islands Dependencies Survey Scientific Reports*, No. 20, 26 pp.

————. 1962. The geology of Antarctica. (*In* WEXLER, H., RUBIN, M. J. *and* J. E. CASKEY, *ed. Antarctic research: the Matthew Fontaine Maury Memorial Symposium.* Washington, D.C., American Geophysical Union, 26–39.) [Geophysical monograph No. 7.]

————. 1964. Stratigraphic correlation in west Antarctica. (*In* ADIE, R. J., *ed. Antarctic geology.* Amsterdam, North-Holland Publishing Company, 307–13.)

AITKENHEAD, N. 1965. The geology of the Duse Bay–Larsen Inlet area, north-east Graham Land (with particular reference to the Trinity Peninsula Series). *British Antarctic Survey Scientific Reports*, No. 51, 62 pp.

ALLEN, A. 1966. Seismic refraction investigations in the Scotia Sea. *British Antarctic Survey Scientific Reports*, No. 55, 44 pp.

ASHCROFT, W. A. 1967. *A seismic refraction study of the crust in the area of Bransfield Strait and the South Shetland Islands in the Scotia arc, South Atlantic.* Ph.D. thesis, University of Birmingham, 226 pp. [Unpublished.]

BARTON, C. M. 1965. The geology of the South Shetland Islands: III. The stratigraphy of King George Island. *British Antarctic Survey Scientific Reports*, No. 44, 33 pp.

BELOUSOV, V. V. 1966. Modern concepts of the structure and development of the Earth's crust and the upper mantle of continents. *Q. Jl geol. Soc. Lond.*, **122**, Pt. 3, No. 487, 293–313.

BIBBY, J. S. 1966. The stratigraphy of part of north-east Graham Land and the James Ross Island group. *British Antarctic Survey Scientific Reports*, No. 53, 37 pp.

BIRCH, F. 1960. The velocity of compressional waves in rocks to 10 kilobars, Part 1. *J. geophys. Res.*, **65**, No. 4, 1083–102.

COOK, K. L. 1962. The problem of mantle-crust mix: lateral inhomogeneity in the uppermost part of the Earth's mantle. (*In* LANDSBERG, H. E. *and* J. VAN MIEGHEM, *ed. Advances in geophysics, Vol. 9.* New York and London, Academic Press, 295–360.)

COX, M. J. G. 1964. Seismic refraction measurements in Bransfield Strait. *British Antarctic Survey Bulletin*, No. 4, 1–12.

DRAKE, C. L. *and* R. W. GIRDLER. 1964. A geophysical study of the Red Sea. *Geophys. J. R. astr. Soc.*, **8**, No. 5, 473–95.

————., EWING, M. *and* G. H. SUTTON. 1959. Continental margins and geosynclines: the east coast of North America north of Cape Hatteras. (*In* AHRENS, L. H., PRESS, F., RANKAMA, K. *and* S. K. RUNCORN, *ed. Physics and chemistry of the Earth*, **3**. London, New York and Paris, Pergamon Press, 110–98.)

ELLIOT, D. H. 1965. Geology of north-west Trinity Peninsula, Graham Land. *British Antarctic Survey Bulletin*, No. 7, 1–24.

————. 1966. Geology of the Nordenskjöld Coast and a comparison with north-west Trinity Peninsula, Graham Land. *British Antarctic Survey Bulletin*, No. 10, 1–43.

EWING, M., WOOLLARD, G. P. *and* A. C. VINE. 1939. Geophysical investigations in the emerged and submerged Atlantic coastal plain. Part III: Barnegat Bay, New Jersey, section. *Bull. geol. Soc. Am.*, **50**, No. 2, 257–96.

FAUST, L. Y. 1951. Seismic velocity as a function of depth and geologic time. *Geophysics*, **16**, No. 2, 192–206.

GRIFFITHS, D. H., RIDDIHOUGH, R. P., CAMERON, H. A. D. *and* P. KENNETT. 1964. Geophysical investigation of the Scotia arc. *British Antarctic Survey Scientific Reports*, No. 46, 43 pp.

GURNEY, J. B. 1964. A geophysical telemetry system. *Lucas Engng Rev.*, **1**, No. 2, 16–23.

HALPERN, M. 1964. Cretaceous sedimentation in the "General Bernardo O'Higgins" area of north-west Antarctic Peninsula. (*In* ADIE, R. J., *ed. Antarctic geology.* Amsterdam, North-Holland Publishing Company, 334–47.)

HAWKES, D. D. 1961*a*. The geology of the South Shetland Islands: I. The petrology of King George Island. *Falkland Islands Dependencies Survey Scientific Reports*, No. 26, 28 pp.

————. 1961*b*. The geology of the South Shetland Islands: II. The geology and petrology of Deception Island. *Falkland Islands Dependencies Survey Scientific Reports*, No. 27, 43 pp.

————. 1962. The structure of the Scotia arc. *Geol. Mag.*, **99**, No. 1, 85–91.

HERDMAN, H. F. P. 1948. Soundings taken during the Discovery Investigations, 1932–39. '*Discovery*' *Rep.*, **25**, 39–106.

HESS, H. H. 1955. Serpentine, orogeny and epeirogeny. (*In* POLDERVAART, A., *ed.* Crust of the Earth. *Spec. Pap. geol. Soc. Am.*, No. 62, 391–407.)

HILL, M. N. 1952. Seismic refraction shooting in an area of the eastern Atlantic. *Phil. Trans. R. Soc.*, Ser. A, **244**, No. 890, 561–94.

————. 1963. Single-ship seismic refraction shooting. (*In* HILL, M. N., *ed. The sea. Ideas and observations on progress in the study of the seas. Vol. 3. The Earth beneath the sea: history.* New York, London, Interscience Publishers, 39–46.)

HOBBS, G. J. 1968. The geology of the South Shetland Islands: IV. The geology of Livingston Island. *British Antarctic Survey Scientific Reports*, No. 47, 34 pp.

KOSMINSKAYA, I. P. *and* Y. V. RIZNICHENKO. 1964. Seismic studies of the Earth's crust in Eurasia. (*In* ODISHAW, H., *ed. Research in geophysics. Vol. 2. Solid earth and interface phenomena.* Cambridge, Mass., Massachusetts Institute of Technology Press, 81–122.)

LAPPIN, M. A. 1966. The field relationships of basic and ultrabasic masses in the basal gneiss complex of Stadlandet and Almklovdalen, Nordfjord, southwestern Norway. *Norsk geol. Tidsskr.*, **46**, Ht. 4, 439–96.

LE PICHON, X. 1968. Sea-floor spreading and continental drift. *J. geophys. Res.*, **73**, No. 12, 3661–97.

MORGAN, W. J. 1968. Rises, trenches, great faults, and crustal blocks. *J. geophys. Res.*, **73**, No. 6, 1959–82.

NAFE, J. E. *and* C. L. DRAKE. 1963. Physical properties of marine sediments. (*In* HILL, M. N., *ed. The sea. Ideas and observations on progress in the study of the seas. Vol. 3. The Earth beneath the sea: history.* New York, London, Interscience Publishers, 794–815.)

OFFICER, C. B., EWING, J. I., HENNION, J. F., HARKRIDER, D. G. *and* D. E. MILLER. 1959. Geophysical investigations in the eastern Caribbean: summary of 1955 and 1956 cruises. (*In* AHRENS, L. H., PRESS, F., RANKAMA, K. *and* S. K. RUNCORN, *ed. Physics and chemistry of the Earth*, **3.** London, New York and Paris, Pergamon Press, 17–109.)

ORLANDO, H. A. 1968. A new Triassic flora from Livingston Island, South Shetland Islands. *British Antarctic Survey Bulletin*, No. 16, 1–13.

PAKISER, L. C. *and* J. S. STEINHART. 1964. Explosion seismology in the Western Hemisphere. (*In* ODISHAW, H. *ed. Research in geophysics. Vol. 2. Solid earth and interface phenomena.* Cambridge, Mass., Massachusetts Institute of Technology Press, 123–47.)

RAITT, R. W. 1957. Seismic refraction studies of Eniwetok attol. *Prof. Pap. U.S. geol. Surv.*, No. 260–S, 685–98.

————. 1963. The crustal rocks. (*In* HILL, M. N., *ed. The sea. Ideas and observations on progress in the study of the sea. Vol. 3. The Earth beneath the sea: history.* New York, London, Interscience Publishers, 85–102.)

RINGWOOD, A. E. *and* D. H. GREEN. 1966. An experimental investigation of the gabbro-eclogite transformation and some geophysical implications. *Tectonophysics*, **3,** No. 5, 383–427.

SHOR, G. G. 1963. Refraction and reflection techniques and procedures. (*In* HILL, M. N., *ed. The sea. Ideas and observations on progress in the study of the seas. Vol. 3. The Earth beneath the sea: history.* New York, London, Interscience Publishers, 20–37.)

TYRRELL, G. W. 1921. A contribution to the petrography of the South Shetland Islands, the Palmer Archipelago, and the Danco Land coast, Graham Land, Antarctica. *Trans. R. Soc. Edinb.*, **53,** Pt. 1, No. 4, 57–79.

————. 1945. Report on rocks from west Antarctica and the Scotia arc. '*Discovery*' *Rep.*, **23,** 37–102.

WORDIE, J. M. 1921. Shackleton Antarctic Expedition, 1914–17: geological observations in the Weddell Sea area. *Trans. R. Soc. Edinb.*, **53,** Pt. 1, No. 2, 17–27.

WORZEL, J. L. 1968. Survey of continental margins. (*In* DONOVAN, D. T., *ed. Geology of shelf seas. Proceedings of the 14th Inter-University Geological Congress.* Edinburgh and London, Oliver & Boyd, 117–54.)

————. *and* G. L. SHURBET. 1955. Gravity interpretations from standard oceanic and continental crustal sections. (*In* POLDERVAART, A., *ed.* Crust of the Earth. *Spec. Pap. geol. Soc. Am.*, No. 62, 87–100.)